frontiers | Frontiers in Energy Research

Recent Advances on Mg–Li–Al Systems for Solid-State Hydrogen Storage: A Review

Noratiqah Sazelee[1], Nurul Amirah Ali[1], Muhammad Syarifuddin Yahya[1], Nurul Shafikah Mustafa[1], Firdaus Abdul Halim Yap[2], Saiful Bahri Mohamed[2], Muhammad Zahruddin Ghazali[3], Suwarno Suwarno[4] and Mohammad Ismail[1]*

[1]*Energy Storage Research Group, Faculty of Ocean Engineering Technology and Informatics, Universiti Malaysia Terengganu, Kuala Nerus, Malaysia,* [2]*Faculty of Innovative Design and Technology, Universiti Sultan Zainal Abidin, Kuala Nerus, Malaysia,* [3]*Casa Armada Sdn. Bhd., Kemaman, Malaysia,* [4]*Department of Mechanical Engineering, Institut Teknologi Sepuluh Nopember (ITS), Surabaya, Indonesia*

The problem of providing compact and safe storage solutions for hydrogen in solid-state materials is demanding and challenging. The storage solutions for hydrogen required high-capacity storage technologies, which preferably operate at low pressures and have good performances in the kinetics of absorption/desorption. Metal hydrides such as magnesium hydride (MgH_2) are promising candidates for such storage solutions, but several drawbacks including high onset desorption temperature (>400°C) and slow sorption kinetics need to be overcome. In this study, we reviewed the recent developments in the hydrogen storage performance development of MgH_2 and found that the destabilization concept has been extensively explored. Lithium alanate or $LiAlH_4$ has been used as a destabilizing agent in MgH_2–$LiAlH_4$ (Mg–Li–Al) due to its high capacity of hydrogen, which is 10.5 wt.%, and low onset desorption temperature (~150°C). In this article, a review of the recent advances in the Mg–Li–Al system for the solid-state hydrogen storage material is studied. We discussed the effect of the ratio of MgH_2 and $LiAlH_4$, milling time, and additives in the Mg–Li–Al system. After the destabilization concept was introduced, the onset of the desorption temperature and activation energy of MgH_2 were reduced, and the sorption properties improved. Further study showed that the intermetallic alloys of $Li_{0.92}Mg_{4.08}$ and $Mg_{17}Al_{12}$ that were formed *in situ* during the dehydrogenation process provide synergetic thermodynamic and kinetic destabilization in the Mg-Li-Al composite system.

De/rehydrogenation measurements indicate that the intermetallic alloys of $Li_{0.92}Mg_{4.08}$ and $Mg_{17}Al_{12}$ were fully reversibly absorbed and desorbed hydrogen. Next, the remaining challenges and a possible development strategy of the Mg–Li–Al system are analyzed. This review is the first systematic study that focuses on the recent advances in the Mg–Li–Al system for storage solutions for hydrogen in solid-state materials.

Keywords: Mg–Li–Al system, magnesium hydride, lithium alanate, hydrogen storage, solid-state storage

INTRODUCTION

Due to global environmental issues and the search for new energy sources and carriers, hydrogen is viewed as the most promising alternative to replace fossil fuel-based energy (Yang et al., 2019; Yao L. et al., 2020; Zhang et al., 2019b). Hydrogen is an environment-friendly energy carrier since it has near-zero greenhouse gas emissions. In addition, hydrogen can also reduce the dependence on imported oil for countries without natural resources (Peláez Peláez et al., 2021; Sartbaeva et al., 2008). Hydrogen is not found naturally, but it can be produced from a variety of primary energy sources (e.g., fossil fuels and biomass) and secondary energy sources (e.g., renewable electricity from wind and hydropower) (Abdin et al., 2020; Thapa et al., 2021). As reported by Dunn (Dunn, 2002), since the mid-19th century, the world has been shifting slowly from one form of energy to another, from solids to liquids and gases, as shown in **Figure 1**. Compared to fossil fuel, hydrogen holds high energy content and can be stored in large quantities over a long time (Satyapal et al., 2007; Sadhasivam et al., 2017). Hydrogen can offer a long-term solution as it can be continuously supplied and can contribute to a variety of automotive fuel sources. As a result, important research and developmental activities are being carried out to improve the efficiency of the hydrogen-based energy system to make it competitive with the existing fossil fuels.

In addition to the lack of infrastructures for hydrogen (for example, production, distribution, and refueling), one of the main roadblocks to the spread of hydrogen is reliable hydrogen storage. Hydrogen-compressed gas tanks, hydrogen liquid tanks, and solid-state storage of hydrogen are possible current approaches to store hydrogen (Sazelee et al., 2018; Doğan et al., 2020). Liquid hydrogen storage systems present a promising opportunity to efficiently increase the capacity of hydrogen fueling stations and are also preferred for space missions (Jiang et al., 2021; Correa-Jullian & Groth, 2022). Although liquid hydrogen tanks are usually super-insulated tanks, at approximately 20 K, boil-off may occur due to the substantial temperature difference between the ambient and liquid hydrogen (Khurana et al., 2006; Zuo et al., 2020). On the other hand, although storage in a compressed gas tank is possible, technical simplicity and the fast filling-releasing rate requires very high pressure and has high costs (Zheng et al., 2012). Therefore, solid-state hydrogen storage draws more attention due to its security, high storage capacity, and hydrogen purification (Niaz et al., 2015; Sazelee et al., 2020b; Ye et al., 2020). However, a drawback of the solid-state hydrogen storage materials, especially for metal/complex hydrides, is their high decomposition temperature and sluggish sorption kinetics (absorb and desorb hydrogen) (Daulbayev et al., 2022).

AN OVERVIEW OF THE Mg–Li–Al SYSTEMS

A wide variety of materials are currently being considered as the future reversible solid-state hydrogen storage materials (Zacharia & Rather, 2015). As claimed by David (David, 2005), the ability to separate hydrogen differs from each metal, and this ability depends on the metals' purity, surface structure, and morphology. The list of the storage systems with their gravimetric capacities is shown in **Table 1**.

Globally, among the solid-state hydrogen storage materials, research into the use of magnesium (Mg) in hydrogen storage applications is of considerable importance (Jain et al., 2010; Crivello et al., 2016; Zhang et al., 2019a; Ouyang et al., 2020). In recent years, much attention has been given to examining the specific material properties of Mg alloys for the development of new functional materials (Yang et al., 2021). Mg is also one of the
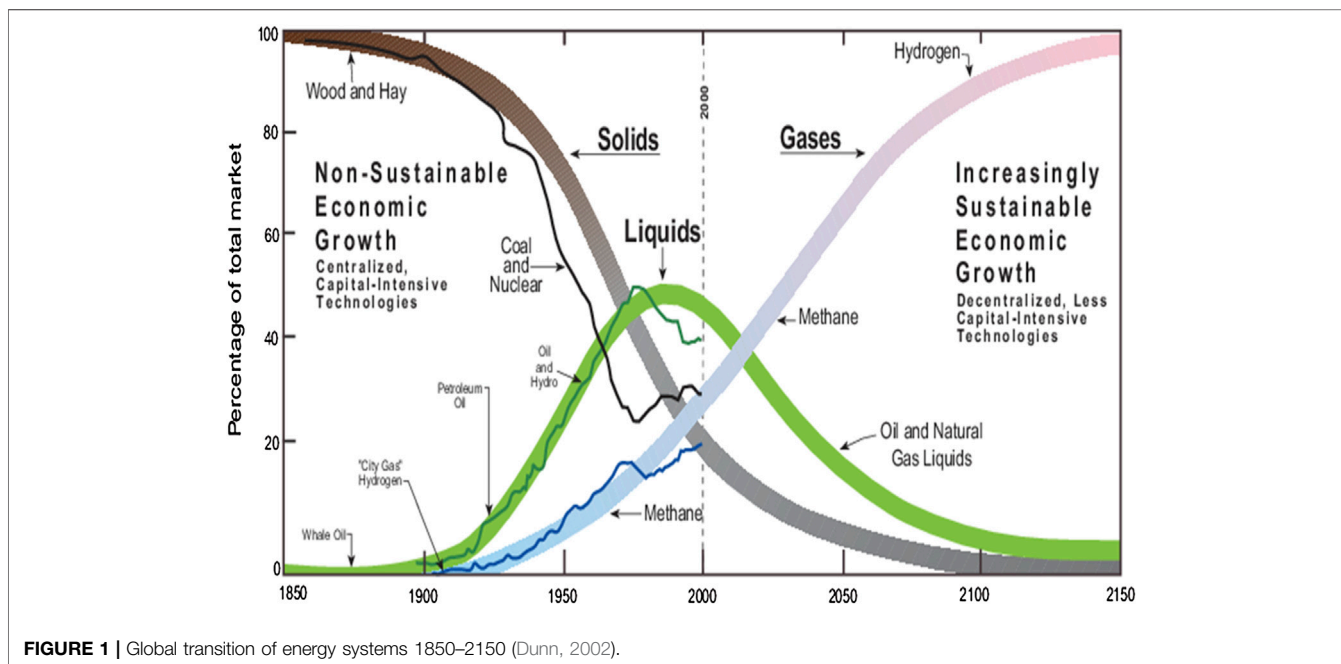

FIGURE 1 | Global transition of energy systems 1850–2150 (Dunn, 2002).

TABLE 1 | Hydride materials and theoretical gravimetric hydrogen density (Kojima, 2019).

Material	Theoretical gravimetric H$_2$ density (wt%)	Materials	Theoretical gravimetric H$_2$ density (wt%)
LiH	12.70	LiBH$_4$	18.5
NaH	4.20	NaBH$_4$	10.7
KH	2.51	KBH$_4$	7.47
MgH$_2$	7.66	Mg(BH$_4$)$_2$	14.8
CaH$_2$	4.79	Ca(BH$_4$)$_2$	11.6
LiAlH$_4$	10.6	LiNH$_2$	8.78
NaAlH$_4$	7.47	NaNH$_2$	5.17
KAlH$_4$	5.75	KNH$_2$	3.66
Mg(AlH$_4$)$_2$	9.34	Mg(NH$_2$)$_2$	7.15
Ca(AlH$_4$)$_2$	7.90	Ca(NH$_2$)$_2$	5.59

most abundant and lightly packed solid materials (1.738 g/cm^3) (Li et al., 2015). Increasing interest in MgH$_2$ has been shown due to its high hydrogen storage capacity (7.6 wt.%), low cost, and superior reversibility (Imamura et al., 2005; Sakintuna et al., 2007; Montone et al., 2010; El Khatabi et al., 2018).

Thus, researchers suggested that hydrogen interaction with Mg is one of the most promising approaches (Eftekhari & Fang, 2017; Luo et al., 2019). While Mg satisfies many practical application requirements, the on-board applications can still not be used for many reasons, such as 1) the desorption/absorption kinetics process is very slow for pure Mg (Schlapbach et al., 1979) and 2) releasing hydrogen at high temperatures (>400°C), is correlated with the high stability of Mg–H bonds and is expressed in the high enthalpy of hydride formation (Zaluska et al., 1999; Dornheim et al., 2007; Jain et al., 2010). To boost MgH$_2$ hydrogen storage properties, numerous techniques have been developed including alloying (Li et al., 2019; Liang et al., 2020; Marques et al., 2020; Dematteis et al., 2021), nanosizing (Ranjbar et al., 2009; Zhang et al., 2015; Yu et al., 2017; Ma et al., 2021), and catalyzing (Polanski et al., 2011; Baricco et al., 2012; Ismail et al., 2016; Jangir et al., 2018; Yao P. et al., 2020; Ismail, 2021; Liu et al., 2021; Lu et al., 2021; Zhang et al., 2021). The remarkable improvements of these techniques have been demonstrated as the most successful methods but still do not fulfill the Department of Energy (DOE) target for solid-state hydrogen storage materials (Urgnani et al., 2008).
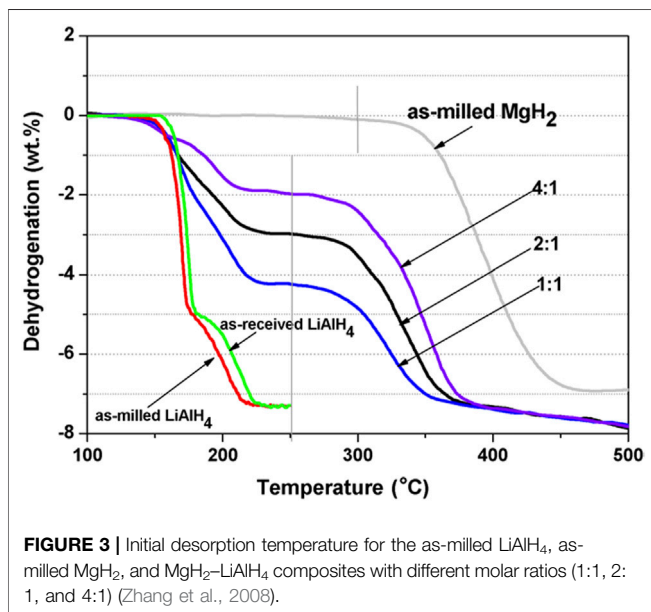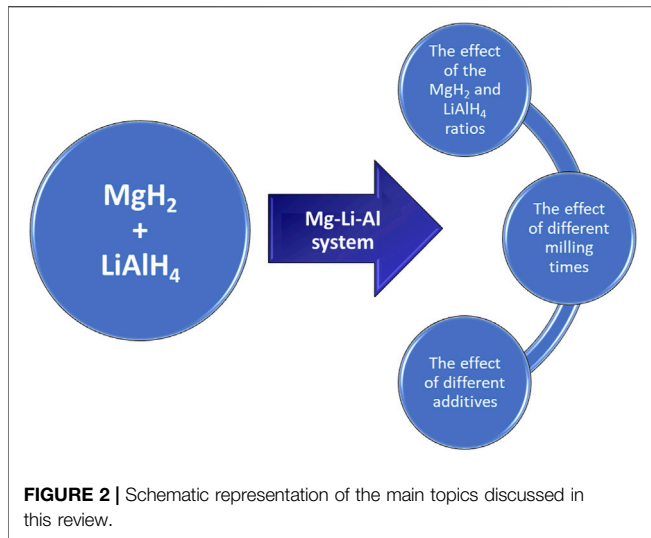
The 'destabilization concept' has been introduced as another method to enhance the sorption kinetics and alter the thermodynamics of MgH$_2$ (Vajo et al., 2004; Vajo et al., 2007; Vajo & Olson, 2007; Ali et al., 2021; Sulaiman et al., 2021b). The concept aims to modify the thermodynamics and kinetics of the hydrogen sorption reaction (Barkhordarian et al., 2007). Thermodynamic destabilization is achieved when the mixed hydrides react and form a new intermediate compound that alters the thermodynamic properties and facilitates hydrogen release and absorption (Reilly & Wiswall, 1968; Ismail & Mustafa, 2016; Ali & Ismail, 2021). Since several studies have been reported on this concept, researchers attempted to destabilize MgH$_2$ by using the reactive hydride composite approach, as in the systems such as MgH$_2$–AlH$_3$ (Liu et al., 2013; Liu et al., 2014; Ismail, 2016), MgH$_2$–Mg(AlH$_4$)$_2$ (Wang et al., 2014), MgH$_2$–NaAlH$_4$ (Ismail et al., 2013; Rafi-ud-din et al.,

2014; Bendyna et al., 2015; Ali & Ismail, 2021), MgH$_2$–NaBH$_4$ (Mao et al., 2009; Kato et al., 2012; Mulas et al., 2012), and other promising destabilizing systems. Among all the destabilizing systems, the researchers tried the destabilizing concept with the most studied materials under the complex hydride, which is LiAlH$_4$, in order to enhance the performance for the practical use of MgH$_2$. Due to its high capacity for storage (10.5 wt.%), LiAlH$_4$ is interesting compared to the other complex hydrides such as NaAlH$_4$ (5.5 wt.%) (Sazelee & Ismail, 2021). LiAlH$_4$ decomposes in three steps (Liu C. et al., 2020). With 5.3 wt.% of H$_2$ at 150°C, the first decomposition occurs as in **Eq. 1**. Meanwhile, the second decomposition occurs at ~180°C (2.6 wt.%), and the third decomposition occurs with a temperature above 350°C (2.6 wt.%), as in **Eqs 2**, **3**, respectively.

$$3LiAlH_4 \rightarrow Li_3AlH_6 + 2Al + 3H_2, \tag{1}$$

$$Li_3AlH_6 \rightarrow 3LiH + Al + 3/2H_2, \tag{2}$$

$$3LiH + 3Al \rightarrow 3LiAl + 3/2H_2. \tag{3}$$
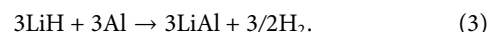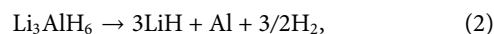
Even though LiAlH$_4$ offers several benefits, it suffers from slow desorption kinetics (hard to release hydrogen at certain conditions), and the last reaction temperature is quite high (Hsu et al., 2014a; Ismail et al., 2021). The enthalpy change of **Eq. 1** is calculated to be −27 kJmol^{-1} (Ke & Chen, 2007), which indicates that the hydrogen evolution from the solid LiAlH$_4$ is thermodynamically allowed at low temperatures but is restricted by a relatively high kinetic barrier in transforming tetrahedron (AlH$_4$)$^-$ to octahedron (AlH$_6$)$^{3-}$ (Chen et al., 2010). All the theoretical and experimental works showed that the LiAlH$_4$ system could absorb hydrogen when a higher hydrogen pressure is applied (more than 8.0 MPa) (Sazelee & Ismail, 2021). This is because LiAlH$_4$ is restricted by weak reversibility and very high thermodynamic stability (Graetz et al., 2008). For instance, Jang et al. (Jang et al., 2006) stated that more than 10^3 bar of hydrogen partial pressure is required for the absorption reaction of Li$_3$AlH$_6$ to LiAlH$_4$ above the room temperature.

To that end, this review concentrated on the destabilized MgH$_2$–LiAlH$_4$ composite (Mg–Li–Al system). This idea is based on the hypothesis that so-called mechano-chemical reactions could occur between MgH$_2$ and LiAlH$_4$, and the intermediate phases (Li$_{0.92}$Mg$_{4.08}$ and Mg$_{17}$Al$_{12}$) could be

FIGURE 2 | Schematic representation of the main topics discussed in this review.

FIGURE 4 | XRD patterns of different ratios of MgH_2 and $LiAlH_4$ in the Mg–Li–Al system after the milling process (Lin & Tsai, 2017).

FIGURE 3 | Initial desorption temperature for the as-milled $LiAlH_4$, as-milled MgH_2, and MgH_2–$LiAlH_4$ composites with different molar ratios (1:1, 2:1, and 4:1) (Zhang et al., 2008).
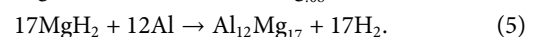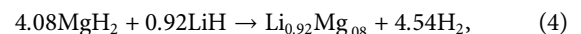
formed to modify the thermal stability of the Mg–Li–Al system. The primary goal of this article is to review the progress of the destabilized MgH_2–$LiAlH_4$ system in improving the performance of MgH_2 and $LiAlH_4$ hydrogen storage. Up to date, no researchers have been reviewing this Mg–Li–Al system. Therefore, we believed that the researchers and practitioners involved in research on hydrogen storage materials will benefit from this review article. **Figure 2** illustrates the main topics discussed in this review.
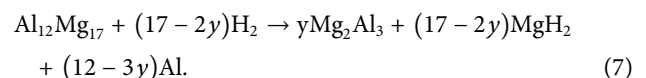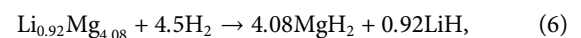
The Effect of the MgH₂ and LiAlH₄ Ratios

The first systematic study on the mutual destabilization between MgH_2 and $LiAlH_4$ was reported by Zhang et al. (Zhang et al., 2008). They studied the different molar ratios (1:1, 2:1, and 4:1) of MgH_2–$LiAlH_4$. The result showed that the initial desorption
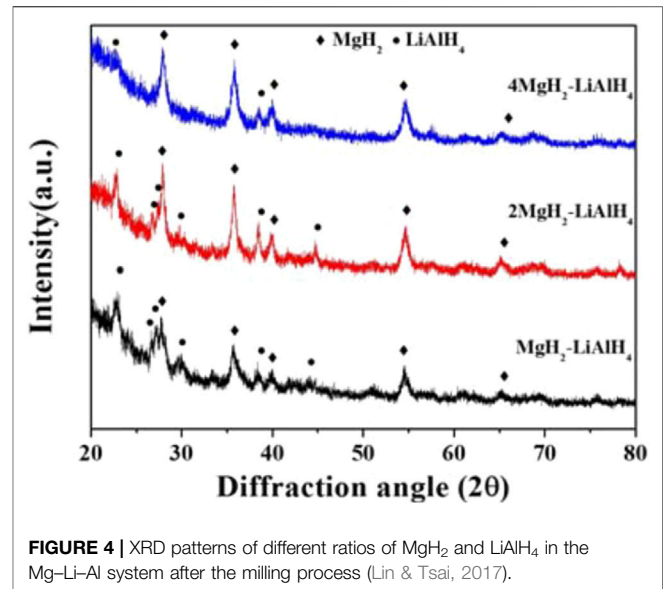
temperature for the MgH_2–relevant decomposition in all the different molar ratios of the MgH_2–$LiAlH_4$ composite was decreased to ~250°C, which is 50°C lower than the milled MgH_2, as shown in **Figure 3**. By using the Kissinger method, the activation energy value of MgH_2–relevant decomposition in the composite was reduced dramatically compared to the undoped MgH_2. The dehydrogenation enthalpies of the MgH_2–$LiAlH_4$ composites with different molar ratios 4:1, 2:1, and 1:1 are 61, 48.66, and 45 kJ/mol, respectively. These enthalpy values were smaller than the undoped MgH_2 (76 kJ/mol), which indicates that MgH_2 was destabilized by $LiAlH_4$. Further study revealed that the dehydrogenation process in the MgH_2–$LiAlH_4$ system can be divided into two steps: the first step is due to the two-step decomposition of $LiAlH_4$ (The first step is the decomposition of $LiAlH_4$ to Li_3AlH_6 and Al (as in **Eq. 1**), and the second step is the decomposition of Li_3AlH_6 to LiH and Al (as in **Eq. 2**) and the second step is due to the reaction between LiH and Al phases to form $Li_{0.92}Mg_{4.08}$ and $Mg_{17}Al_{12}$ phases, as indicated in **Eqs 4**, **5**.

$$4.08MgH_2 + 0.92LiH \rightarrow Li_{0.92}Mg_{08} + 4.54H_2, \quad (4)$$

$$17MgH_2 + 12Al \rightarrow Al_{12}Mg_{17} + 17H_2. \quad (5)$$

Moreover, rehydrogenation measurement shows that $Li_{0.92}Mg_{4.08}$ and $Mg_{17}Al_{12}$ are the fully absorbed hydrogen, as shown in **Eqs 6**, **7**.

$$Li_{0.92}Mg_{4.08} + 4.5H_2 \rightarrow 4.08MgH_2 + 0.92LiH, \quad (6)$$

$$Al_{12}Mg_{17} + (17 - 2y)H_2 \rightarrow yMg_2Al_3 + (17 - 2y)MgH_2$$
$$+ (12 - 3y)Al. \quad (7)$$

Lin and Tsai (Lin & Tsai, 2017) in their study exposed that the diffraction peak intensity of $LiAlH_4$ decreased with an increasing amount of MgH_2 addition, as in **Figure 4**. No other compounds were found after milling, indicating that no reaction occurred

TABLE 2 | TGA results show the temperature of desorption and the amount of hydrogen absorption/desorption from MgH_2–$LiAlH_4$ with different amounts of composites (Lin & Tsai, 2017).

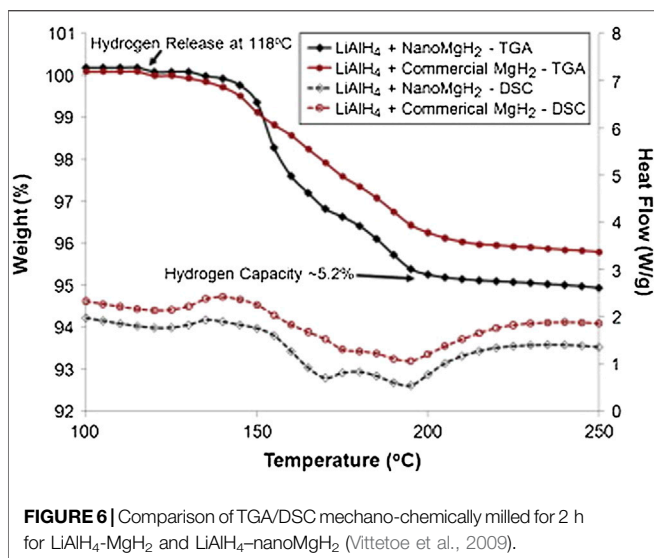| Composite	First onset desorption temperature (˚C)	Amount of hydrogen released (wt%)	Amount of hydrogen absorbed (wt%)
MgH_2–$LiAlH_4$	100	5.3	0.3
$2MgH_2$–$LiAlH_4$	100	5.0	1.3
$4MgH_2$–$LiAlH_4$	85	5.3	3.0
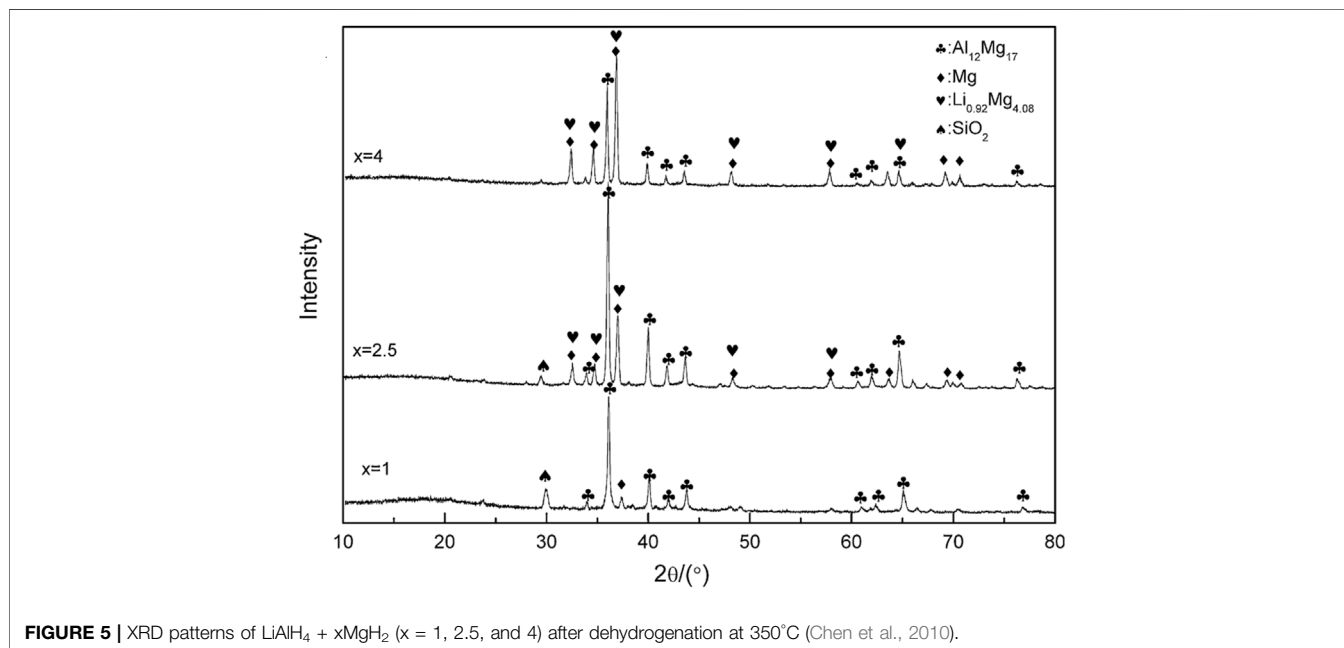
FIGURE 5 | XRD patterns of $LiAlH_4$ + $xMgH_2$ (x = 1, 2.5, and 4) after dehydrogenation at 350˚C (Chen et al., 2010).

between $LiAlH_4$ and MgH_2 during the milling process. This result is in agreement with a previous study by Hsu et al. (Hsu et al., 2014b), in which the diffraction peak intensity of MgH_2 increased with a decreasing amount of $LiAlH_4$ in the MgH_2–$LiAlH_4$ mixture.

Next, the temperatures of desorption and the amount of hydrogen released from the composites of MgH_2–$LiAlH_4$ were quantitively evaluated by the thermogravimetric analysis (TGA), as shown in **Table 2**. It was evident that with the increasing MgH_2 content in the composites, the first desorption temperature was lowered. These findings showed that MgH_2 played an effective role in reducing the initial desorption temperature of these composites. As soon as the desorption of these composites was completed, absorption kinetics was initiated with a temperature maintained at 400˚C, while charging hydrogen to the target pressure. As displayed in **Table 2**, the total amount of hydrogen absorbed (wt.%) increased from 0.3 to 3, and the onset desorption temperature also decreased to 85˚C compared to 100˚C with an increase in the MgH_2 content in the composites. The results proved that MgH_2 was the main compound that exhibited reversibility concerning the hydrogen absorption/desorption reaction. As shown in **Table 2**, the ability of the MgH_2–$LiAlH_4$ composite to absorb hydrogen increased as the MgH_2 ratio increased.

The $LiAlH_4$–MgH_2 hydrogen storage system was studied by Chen et al. (Chen et al., 2010). The commercial $LiAlH_4$ was decomposed at 163˚C; meanwhile, the commercial MgH_2 decomposed at 405˚C. However, $LiAlH_4$ and MgH_2 mixtures start to release hydrogen at ~107˚C, indicating that the combination of $LiAlH_4$ and MgH_2 may improve their thermodynamic properties. Measurement of the XRD was performed after desorption, and the results showed that in all the $LiAlH_4$–$xMgH_2$ composites ($LiAlH_4$–MgH_2, $LiAlH_4$–$2.5MgH_2$, and $LiAlH_4$–$4MgH_2$), the $Mg_{17}Al_{12}$ phase was formed. In addition, the $LiAlH_4$–$4MgH_2$ composite contained major $Li_{0.92}Mg_{4.08}$ phases, whereas $LiAlH_4$–$2.5MgH_2$ contained minor $Li_{0.92}Mg_{4.08}$ phases, as shown in **Figure 5**. This indicates that $Li_{0.92}Mg_{4.08}$ can be formed while the ratio of MgH_2/$LiAH_4$ is relatively high. These composites also undergo an absorption process at 350˚C under a pressure of 10 MPa hydrogen. In 60 min, the $LiAlH_4$–$4MgH_2$ composites reach 90% of their maximum absorption capacity. In brief, these reported studies indicated that the combination of $LiAlH_4$ and MgH_2 may have been shown to affect the thermal stability of both $LiAlH_4$ and MgH_2 by the formation of intermetallic $Mg_{17}Al_{12}$ and $Li_{0.92}Mg_{4.08}$.

Based on the abovementioned discussions, the different molar ratios of the MgH_2–$LiAlH_4$ composites also affected the

FIGURE 6 | Comparison of TGA/DSC mechano-chemically milled for 2 h for LiAlH$_4$-MgH$_2$ and LiAlH$_4$–nanoMgH$_2$ (Vittetoe et al., 2009).

performance of the Mg–Li–Al system. This review article outlined that 4MgH$_2$–LiAlH$_4$ shows the best performance compared to the other ratios (e.g., 1:1, 2:1, and 2.5:1). The 4MgH$_2$–LiAlH$_4$ composite created an intermediate compound of Li$_{0.92}$Mg$_{4.08}$ and Mg$_{17}$Al$_{12}$ that helps to enhance the hydrogen storage performance of the Mg–Li–Al system.
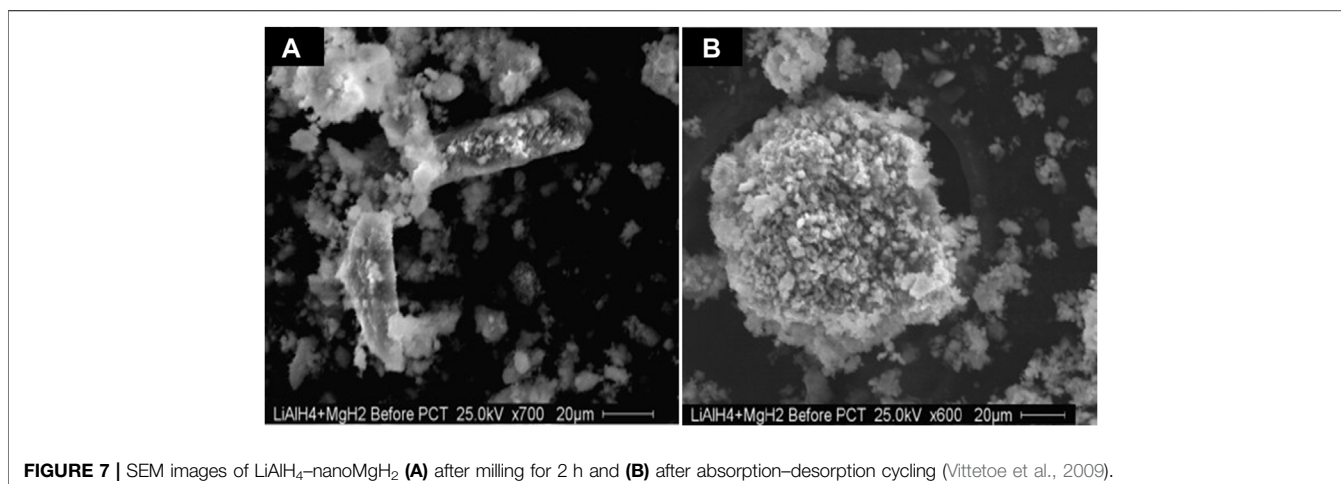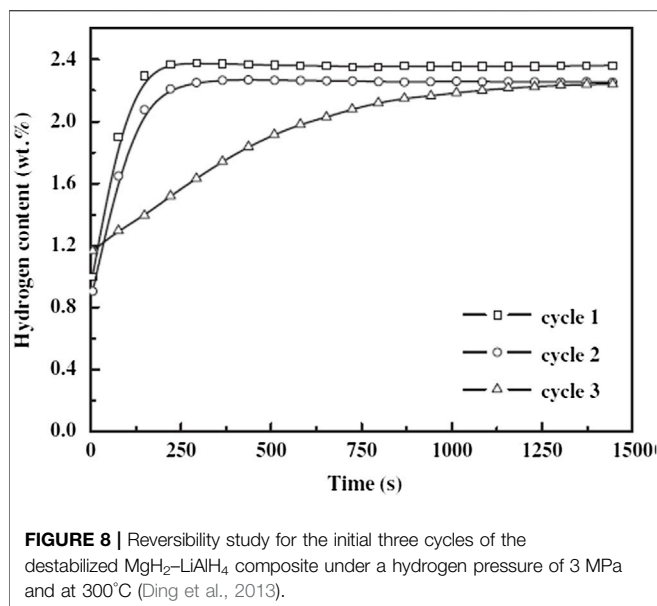
The Effect of Different Milling Times

Vittetoe et al. (Vittetoe et al., 2009) explored the destabilization effects of the combination of LiAlH$_4$ with a nanocrystalline MgH$_2$ by mechanical–chemical milling concerning reversibility and kinetics problems. Interestingly, they investigated the LiAlH$_4$–MgH$_2$ composite with different durations of milling (1, 2, 3, and 5 h). They discovered that the LiAlH$_4$–MgH$_2$ samples that have been milled for 1, 2, and 3 h started to decompose at ~100°C. Researchers verified that for an optimal ball milling period of 2 h, a three-step hydrogen desorption response with an early-onset temperature and greater amount of hydrogen release is required. In addition, further study

elucidates LiAlH$_4$–MgH$_2$ and LiAlH$_4$–nanoMgH$_2$ of TGA and differential scanning calorimetry (DSC) profiles milled for 2 h, as seen in **Figure 6**. The LiAlH$_4$–nanoMgH$_2$ systems show a greater weight loss of approximately 5.2 wt.% (~200°C), at least 1.0 wt.% higher capacity than the commercial-grade sample (LiAlH$_4$–MgH$_2$).

As LiAlH$_4$–nanoMgH$_2$ showed better performance than LiAlH$_4$–MgH$_2$, this material underwent repeated absorption of hydrogen (80 bars) and desorption at two different temperatures (300 and 350°C). After numerous attempts of hydrogen absorption–desorption experiments, these samples were carefully examined under a scanning electron microscope (SEM), as shown in **Figure 7**. SEM images of LiAlH$_4$–nanoMgH$_2$ after cycling indicated that the sample had a relatively smaller grain with a highly porous matrix and uniform (as in **Figure 7B**) as compared to LiAlH$_4$–nanoMgH$_2$ (as in **Figure 7A**). This is due to the host structure's effective uptake and release of hydrogen.

Milanovic et al. (Milanović et al., 2013) investigated the catalytic influence on the desorption of hydrogen from MgH$_2$. Indeed, when mixing MgH$_2$ with a 5 wt.% of LiAlH$_4$ for 15 min, the peak of the hydrogen desorption shifts to a lower temperature than as received MgH$_2$ and as milled MgH$_2$. In this study, milling up to 30 and 60 min of the MgH$_2$–LiAlH$_4$ composites may reduce the catalytic activity of the LiAlH$_4$ additive, as revealed by the shift to a higher peak of desorption temperatures. According to Leon et al. (Léon et al., 2009), experiments conducted under various conditions revealed that the milling parameters, in particular the milling speed and milling time, can be of great importance through reactive ball milling for the formation of the new hydride phase. Next, Ding et al. (Ding et al., 2013) studied the MgH$_2$–LiAlH$_4$ composites milled at different milling times (2, 5, and 9 h). The result revealed that MgH$_2$–LiAlH$_4$ composites milled for 2 h decompose in the temperature ranges of ~130–183°C; meanwhile, after the MgH$_2$–LiAlH$_4$ composites were milled for 5 h, the composites start to release hydrogen at 102°C. However, the capacity of hydrogen released decreased compared with 2 h milled composites. In addition to that, the initial desorption temperature decreases to 86°C when the milling

FIGURE 7 | SEM images of LiAlH$_4$–nanoMgH$_2$ **(A)** after milling for 2 h and **(B)** after absorption–desorption cycling (Vittetoe et al., 2009).

FIGURE 8 | Reversibility study for the initial three cycles of the destabilized MgH$_2$–LiAlH$_4$ composite under a hydrogen pressure of 3 MPa and at 300°C (Ding et al., 2013).

time increases to 9 h, but the amount of hydrogen released also decreases. The XRD pattern showed that the peaks of Li$_3$AlH$_6$ and Al appeared after milling the MgH$_2$–LiAlH$_4$ composites up to 5 h. Interestingly, milling up to 9 h proved that the intensity peaks of Li$_3$AlH$_6$ and Al become stronger. This indicated that more LiAlH$_4$ has been decomposed into Li$_3$AlH$_6$ and Al, accounting for the lowest onset desorption temperature. Based on the results obtained, the lower decomposition temperature was attributed to the decomposition of LiAlH$_4$ that had occurred, and more LiAlH$_4$ decomposed as the milling time increased. In addition, the peaks of the Mg$_{17}$Al$_{12}$ phase can also be detected when the MgH$_2$–LiAlH$_4$ composites were heated to 250°C. Furthermore, Ding et al. (Ding et al., 2013) also studied the reversibility of the destabilized MgH$_2$–LiAlH$_4$ composite under a hydrogen pressure of 3 MPa and at 300°C, and the results show that the MgH$_2$–LiAlH$_4$ composite exhibits fast ab/desorption kinetics in the first two cycles, but the ab/desorption kinetics worsened during the third cycle, as shown in **Figure 8**. Moreover, SEM images indicated that the morphology of MgH$_2$–LiAlH$_4$ composites was smaller. A reduction in the particle size and crystallite size results in the introduction of high surface defect density and the creation of more grain boundaries. In addition to that, a high density of the nanosized catalyst particles forms a large number of nucleation sites at the surface of the LiAlH$_4$ matrix, leading to the larger surface area of LiAlH$_4$ particles, as indicated by Zhai et al. (Zhai et al., 2012). Xia et al. (Xia et al., 2020) also stated that the morphological change should be beneficial for the enhancement of the desorption properties of LiAlH$_4$, owing to the reduction of the particle size and the process of creating small crystallite sizes. Halim Yap et al. (Halim Yap et al., 2019), in their study, revealed that the decrement of the grain sizes led to the increment of the contact surface area. As a result, the desorption reaction of hydrogen has been improved due to the reduction of the hydrogen diffusion length. A study conducted by Czujko et al. (Czujko et al., 2011) revealed that the

average particle size of MgH$_2$+50 wt% LiAlH$_4$ composites was reduced to ~3.5 ± 2.7 μm. It demonstrated that during MgH$_2$ ball milling, lithium alanate could act as a lubricant, and the reduction of particle size is much less efficient when the LiAlH$_4$ additive level reaches 50 wt.%. Based on this subsection, appropriate milling time is beneficial to the Mg–Li–Al systems. This indicates that the milling time at a suitable time is helpful to improve the hydrogen storage performance of the Mg–Li–Al system. The variation of the milling duration has obvious effects on the onset desorption temperature, activation energy, and morphology of the samples.

The Effect of Different Additives

A study conducted by Halim Yap and Ismail (Halim Yap & Ismail, 2017) indicated that the hydrogen sorption properties of the MgH$_2$–LiAlH$_4$ system can be enhanced by the addition of K$_2$ZrF$_6$. The onset desorption temperature for 4MgH$_2$–LiAlH$_4$ exhibited two significant stages. For the 4MgH$_2$–LiAlH$_4$ systems, the onset desorption temperature was 135 and 275°C for the first and second desorption stages, with the total amount of hydrogen desorption being 7.5 wt.%. After the addition of 10 wt.% K$_2$ZrF$_6$, the desorption temperature for the first and second stages was decreased by 40 and 25°C, respectively. In addition, 4MgH$_2$–LiAlH$_4$ + 10 wt.% K$_2$ZrF$_6$ demonstrates better kinetics of desorption, and the value of activation energy was decreased to 102.9 kJ/mol compared to the undoped composites (129.8 kJ/mol). However, the absorption kinetics under 33.0 atm at 320°C exposed that adding 10 wt.% of K$_2$ZrF$_6$ to 4MgH$_2$–LiAlH$_4$ showed no improvement in the absorption of hydrogen. Meanwhile, the SEM images for comparing the morphology of undoped and doped samples are shown in **Figure 9**. The doped samples show that the particles size is less agglomerated and smaller as in **Figure 9D** than the undoped samples (**Figure 9C**). This result was also supported by Ranjbar et al. (Ranjbar et al., 2010) who suggested that the smaller particle size improves hydrogen ab/desorption as it makes the particle larger surface area and reduces the diffusion length of hydrogen.

Further research indicated that the new peaks of Al$_3$Zr and KH (indicating LiAlH$_4$ react with K$_2$ZrF$_6$) were formed after 4MgH$_2$–LiAlH$_4$ + 10 wt.% K$_2$ZrF$_6$ were heated at 200°C. In addition, the peaks of MgH$_2$ were also present as well as LiH and Al (illustrated the decomposition as in **Eq. 2**). Heating up to 450°C, the peaks of Mg, Li$_{0.92}$Mg$_{4.08}$, and Mg$_{17}$Al$_{12}$ were detected, whereas the Al$_3$Zr and KH peaks remained unchanged. Furthermore, the XRD pattern of absorption for K$_2$ZrF$_6$-doped 4MgH$_2$–LiAlH$_4$ sample at 300°C also exposed the peaks of Al$_3$Zr, KH, LiH, and Al remain unchanged. However, the peaks of the Mg$_{17}$Al$_{12}$ and Li$_{0.92}$Mg$_{4.08}$ disappeared, and it is suggested that a reaction occurred during the absorption process, as indicated in **Eqs 6, 7**. The amount of K$_2$ZrF$_6$ was increased to 20 wt.% to obtain a better insight into the F-containing, Zr-containing, and K-containing phase structures. New minor peaks attributed to LiF were detected along with the KH and Al$_3$Zr phases. Therefore, it is recognized that the new LiF, KH, and Al$_3$Zr products created during the heating process worked together as active components to work on improving the 4MgH$_2$–LiAlH$_4$ system of the hydrogen storage performance. The hydrogen storage
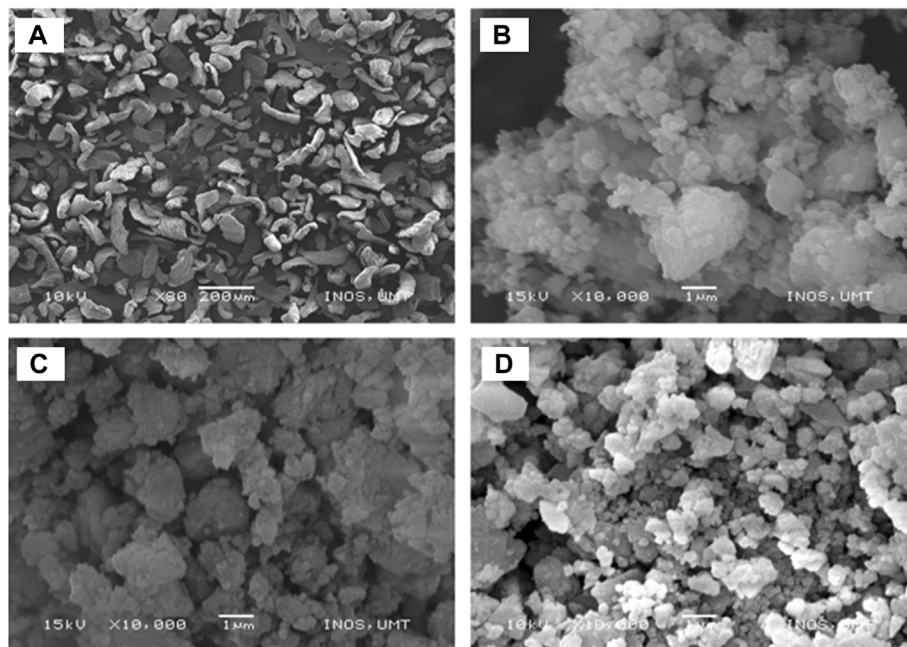
FIGURE 9 | SEM images for the **(A)** as-received MgH₂, **(B)** as-milled MgH₂, **(C)** 4MgH₂-LiAlH₄, and **(D)** 4MgH₂-LiAlH₄ + 10 wt.% K₂ZrF₆ (Halim Yap & Ismail, 2017).

properties of MgH_2/$LiAlH_4$ were improved by the addition of $SrFe_{12}O_{19}$, as suggested by Sulaiman and Ismail (Sulaiman & Ismail, 2017). The result disclosed that the addition of 5 wt.% of $SrFe_{12}O_{19}$ resulted in a decrease of 40 and 10°C in the first and second stages of desorption, respectively, compared to the MgH_2/$LiAlH_4$ system. The doped samples begin to release hydrogen at ~80°C for the first stages and ~260°C for the second stages. Interestingly, the hydrogen released by the doped samples was 7.1 wt.%, which is the amount of hydrogen released equivalent to milled MgH_2. The energy barriers for the release of hydrogen affected the kinetic desorption performance of the samples. From the calculation of as-received MgH_2, the activation energy was 175 kJ/mol. However, the activation energy was decreased to 133 kJ/mol after MgH_2 was milled for 1 h. This proves that the value of the activation energy is also affected by the milling process (Sabitu & Goudy, 2012; Ismail, 2015; Lin et al., 2015; Zhang et al., 2017). Furthermore, after destabilizing MgH_2 with $LiAlH_4$, the activation energy was reduced to 121 kJ/mol, which showed a reduction of 12 kJ/mol compared to the milled MgH_2 (133 kJ/mol). The improvement of desorption kinetics is related to the energy barrier for the hydrogen release from the composite. Lower activation energy means faster kinetics. In this context, the activation energy is the least energy required to instigate the decomposition process of the system (Ismail et al., 2020). The activation energy decreased to 104 kJ/mol, after the addition of 5 wt.% $SrFe_{12}O_{19}$ to $4MgH_2$–$LiAlH_4$. Furthermore, these findings appear to be comparable to the previous studies reporting on the role of catalysts in reducing the activation energy, leading to improved dehydriding kinetics (Sazelee et al., 2019). Conversely, the newly developed products formed during

the heating process of *in situ* $Li_2Fe_3O_4$ and Al_2Sr exhibit a synergistically catalytic effect on the improvement of the $4MgH_2$–$LiAlH_4$ composites.

According to Mao et al. (Mao et al., 2011), dehydrogenation has been improved after $LiAlH_4$ was combined with MgH_2, in which the first-stage desorption temperature is close to $LiAlH_4$ (~150°C), while the second-stage desorption was completed at 233°C. This suggested that in the binary $LiAlH_4$–MgH_2 system, a mutual destabilization occurred. However, after being doped with TiF_3, hydrogen starts to release at ~60°C (100°C lower than the undoped $LiAlH_4$–MgH_2 system). The desorption and absorption kinetics were also improved after the addition of TiF_3. For the $LiAlH_4$–MgH_2–TiF_3 system, the amount of hydrogen desorbed was 2.48 wt.% after 10 min, compared to the $LiAlH_4$–MgH_2 system (1.59 wt.%) at 300°C. Furthermore, the reversibility of this system was performed at 300°C under ~2 MPa for both samples. $LiAlH_4$–MgH_2–TiF_3 systems demonstrate the ability to absorb 2.68 wt.% hydrogen after 5 min, which is greater than the $LiAlH_4$–MgH_2 system (1.75 wt.%). Further study showed that the intermediate phase of $Mg_{17}Al_{12}$ and Li_3Mg_7 produced during the heating process is mainly due to the Al/LiH reaction with MgH_2, as shown in **Eqs 5, 8**:

$$3LiH + 7MgH_2 \rightarrow Li_3Mg_7 + 8.5H_2. \qquad (8)$$
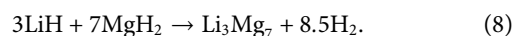
The hydrogen sorption properties of $4MgH_2$–$LiAlH_4$ were greatly improved after the addition of 5 wt.% Fe_2O_3, as eloquently stated by Mustafa et al. (Mustafa & Ismail, 2014). As-milled MgH_2 can release hydrogen at 350°C; meanwhile, the as-milled $LiAlH_4$ can release at 135–160°C. For the destabilized system of $4MgH_2$–$LiAlH_4$, the onset desorption temperature was reduced similar to the as-milled

Composite	Onset desorption temperature (°C)			Total amount of hydrogen released (wt%)
	First stage	Second stage	Third stage	
MgH$_2$–LiAlH$_4$	140	220	340	6.71
MgH$_2$–LiAlH$_4$ + 1 mol% MnFe$_2$O$_4$	110	205	325	6.82
MgH$_2$–LiAlH$_4$ + 3 mol% MnFe$_2$O$_4$	90	195	310	6.78
MgH$_2$–LiAlH$_4$ + 5 mol% MnFe$_2$O$_4$	55	170	300	6.74
MgH$_2$–LiAlH$_4$ + 7 mol% MnFe$_2$O$_4$	53	160	270	5.04

LiAlH$_4$. However, after the addition of Fe$_2$O$_3$, the onset of desorption was decreased to 95°C. The desorption and absorption kinetics were also improved after the addition of Fe$_2$O$_3$. The apparent activation energy of 4MgH$_2$–LiAlH$_4$ + Fe$_2$O$_3$ was reduced to 117 kJ/mol compared to the undoped 4MgH$_2$–LiAlH$_4$ systems. Further research exposed that the Li$_2$Fe$_3$O$_4$ was developed by heating 4MgH$_2$–LiAlH$_4$ + Fe$_2$O$_3$ up to 400°C and revealed that the Li$_2$Fe$_3$O$_4$ also plays a crucial role in reducing the value of desorption temperature and activation energy in the 4MgH$_2$–LiAlH$_4$ systems.

According to Wan et al. (Wan et al., 2013), the hydrogen storage performance of MgH$_2$–LiAlH$_4$ was effectively improved after the addition of MnFe$_2$O$_4$ nanoparticles. As indicated in **Table 3**, the onset desorption temperature for MgH$_2$–LiAlH$_4$ + 5 mol% of MnFe$_2$O$_4$ and MgH$_2$–LiAlH$_4$ + 7 mol% of MnFe$_2$O$_4$ revealed the lowest onset desorption temperature. However, the total amount of hydrogen released for MgH$_2$–LiAlH$_4$ + 5 mol% of MnFe$_2$O$_4$ is higher than the addition of 7 mol% of MnFe$_2$O$_4$. Nonetheless, the addition of MnFe$_2$O$_4$ can reduce the onset desorption temperature of the MgH$_2$–LiAlH$_4$ systems.

For the desorption kinetics at 200°C, under 0.1 MPa, the MgH$_2$–LiAlH$_4$ systems release 0.94 wt.% hydrogen, whereas the MgH$_2$–LiAlH$_4$ + 5 mol% of MnFe$_2$O$_4$ can release 2.91 wt.%. Furthermore, the reversibility for those samples was investigated at 300°C under 3 MPa, and the doped samples show better absorption kinetics than the undoped samples. For MgH$_2$–LiAlH$_4$ + 5 mol% of MnFe$_2$O$_4$, a hydrogen absorption capacity of 3.64 wt.% was achieved within 300 s. In the meantime, the MgH$_2$–LiAlH$_4$ systems only absorbed 2.81 wt.% of hydrogen under the same conditions. Moreover, after heating up to 400°C, the XRD pattern shows the peaks of Li$_{0.92}$Mg$_{4.08}$ and Mg$_{17}$Al$_{12}$. Furthermore, the new peak of Fe$_{0.872}$O observed also indicated that the interaction between LiAlH$_4$ and MnFe$_2$O$_4$ had occurred. However, no Mn-containing peak has been seen due to the low amount of MnFe$_2$O$_4$ that has been used. Also, the XRD pattern observed after the absorption kinetics at 300°C stated that no peaks of Li$_{0.92}$Mg$_{4.08}$ and Mg$_{17}$Al$_{12}$ have been detected. The peaks of Fe$_{0.872}$O can still be seen in the XRD pattern of the absorption results. Therefore, they concluded that the *in situ* formed Fe oxide and the Mn-containing peak enhanced hydrogen storage performances of the MgH$_2$–LiAlH$_4$ system.
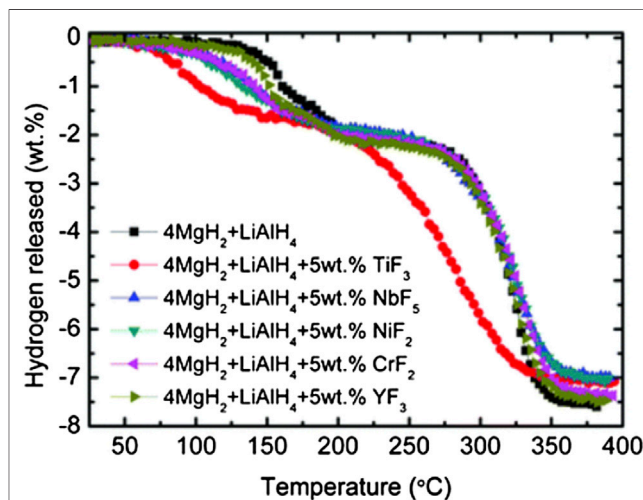
FIGURE 10 | Decomposition temperature results of the MgH$_2$-LiAlH$_4$ composite with different selected metal halides (Ismail et al., 2011).

The impact of various additives on the hydrogen storage properties of the MgH$_2$-LiAlH$_4$ system was studied by Ismail et al. (Ismail et al., 2011). Milled MgH$_2$ starts to decompose at 330°C and desorb about 7.1 wt.% of hydrogen at 420°C. Meanwhile, the as-milled LiAlH$_4$ decomposes at ~142°C for the first and ~173°C for the second stage. After the two hydrides (MgH$_2$–LiAlH$_4$) with ratio 4:1 have been mixed, the samples began to decompose at 130°C for the first stage (attributed to the decomposition of LiAlH$_4$), while at 270°C for the second stages (corresponding to the decomposition of Li$_3$AlH$_6$). The 4MgH$_2$–LiAlH$_4$ was completed at ~360°C with 7.5 wt.% of hydrogen released (attributed to the decomposition of MgH$_2$). After the addition of metal halides, the temperature-programmed desorption (TPD) curves of 4MgH$_2$–LiAlH$_4$ systems were significantly improved. TiF$_3$ followed by NiF$_2$, CrF$_2$, NbF$_5$, and YF$_3$ showed a strong catalytic influence on the decomposition of MgH$_2$–LiAlH$_4$, as shown in **Figure 10**. The MgH$_2$–LiAlH$_4$ composite doped with TiF$_3$ begins to decompose at 70°C. However, the desorption kinetics of the MgH$_2$–LiAlH$_4$ composite were significantly enhanced after the addition of 5 wt.% of metal halides. Furthermore, the addition of metal halide additives could reduce the activation energy of the MgH$_2$–LiAlH$_4$ composite. The

TABLE 4 | Apparent activation energy for the MgH$_2$-LiAlH$_4$ composite with different selected metal halides (Ismail et al., 2011).

Composite	Activation energy (kJ/mol)
4MgH$_2$–LiAlH$_4$	126
4MgH$_2$–LiAlH$_4$ + TiF$_3$	83
4MgH$_2$–LiAlH$_4$ + NbF$_5$	110
4MgH$_2$–LiAlH$_4$ + NiF$_2$	120

apparent activation energy for the MgH$_2$–LiAlH$_4$ composite with the selected different metal halides is shown in **Table 4**.

In order to study the phase structure of these samples, the 4MgH$_2$–LiAlH$_4$ samples were characterized by using XRD. After the samples were heated up to 400°C, apart from Mg, the intermediate phases of Li$_{0.92}$Mg$_{4.08}$ and Al$_{12}$Mg$_{17}$ were eventually created in the composite system. The XRD measurements were also carried out on the absorption kinetics. The results showed that the peaks of Li$_{0.92}$Mg$_{4.08}$ and Al$_{12}$Mg$_{17}$ disappeared; meanwhile, the appearance of peaks of Al$_3$Mg$_2$ indicated that the reaction, as in **Eqs 6, 7**, occurred during the absorption process. For the doped samples, further research showed that LiF and Al$_3$Ti are believed to act as the actual catalyst that can enhance the interaction of the MgH$_2$–LiAlH$_4$ system, while speeding up the hydrogen desorption process of the MgH$_2$–LiAlH$_4$ system. According to Mustafa et al. (Mustafa et al., 2015), the addition of K$_2$TiF$_6$ improves the 4MgH$_2$–LiAlH$_4$ system of hydrogen storage performance. The desorption temperature of the 4MgH$_2$–LiAlH$_4$ system was reduced to 80 and 250°C for the first and second stages, respectively, after the addition of K$_2$TiF$_6$. Meanwhile, the 4MgH$_2$–LiAlH$_4$ composite decomposed at 130 and 270°C for the first and second stages, respectively. In addition, after the addition of K$_2$TiF$_6$, desorption and absorption kinetics were also enhanced. The activation energy for 4MgH$_2$–LiAlH$_4$ systems has also been reduced from 126 to 107 kJ/mol. The XRD analysis was conducted on 4MgH$_2$–LiAlH$_4$ + K$_2$TiF$_6$ for the possible reaction of catalytic additives on the 4MgH$_2$–LiAlH$_4$ systems. The intermediate phases of Li$_{0.92}$Mg$_{4.08}$, Al$_{12}$Mg$_{17}$, and Mg were eventually formed after desorption at 400°C. The complete recovery of LiH and MgH$_2$ from the Li–Mg and Al–Mg alloys was accomplished in the absorption samples due to the reaction of Al$_{12}$Mg$_{17}$ and Li$_{0.92}$Mg$_{4.08}$ with hydrogen. Further verification stated that the peaks of TiH$_2$, LiF, and Al$_3$Ti act as the real catalyst, thus proving that the addition of K$_2$TiF$_6$ enhanced the sorption properties of the 4MgH$_2$–LiAlH$_4$ systems.

Recently, Sulaiman et al. (Sulaiman et al., 2021a) observed an improvement in the onset desorption temperature and the morphology of the 4MgH$_2$–LiAlH$_4$ systems when 5 wt.% of Al$_2$TiO$_5$ was added. The hydrogen started to release at 85°C which is decreased by 35°C for the undoped systems. It is important to note that the inclusion of Al$_2$TiO$_5$ to the 4MgH$_2$–LiAlH$_4$ systems resulted in significantly smaller particle sizes which help to shorten the diffusion length and larger nucleation sites. Moreover, based on the XRD result, the

new *in situ* active species of LiTi$_2$O$_4$, TiH$_2$, and AlTi$_2$ were detected after the de/rehydrogenation process which is believed to act as a true catalyzer in improving the hydrogen storage performance of the Al$_2$TiO$_5$-doped Mg–Li–Al systems. From the results, it is noted that the addition of additives ameliorates the performance of the MgH$_2$–LiAlH$_4$ composite by reducing the onset decomposition temperature and fastening the sorption kinetics performance than the unary MgH$_2$ and LiAlH$_4$, as demonstrated in **Table 5**. **Table 5** presents the onset desorption temperature, total desorption, absorption capacity, and activation energy for the MgH$_2$–LiAlH$_4$ system doped with several additives. The undoped MgH$_2$, LiAlH$_4$, and MgH$_2$–LiAlH$_4$ systems are also included in **Table 5** for comparison purposes.

Based on the abovementioned discussion and **Table 5**, it can be stated that the addition of the additives significantly enhanced the hydrogen storage performance of the MgH$_2$–LiAlH$_4$ systems. It is reported that the active species that are *in situ* formed during the heating process are believed to play a catalytic role in enhancing the hydrogen sorption performance of the MgH$_2$–LiAlH$_4$ additive system. Up to this date, the addition of MnFe$_2$O$_4$ to Mg–Li–Al composites has presented the best performance which can release hydrogen approximately at 55°C (Wan et al., 2013). In addition, the MgH$_2$–LiAlH$_4$–MnFe$_2$O$_4$ system can absorb 3.64 wt.% of hydrogen in only 300 s and desorb more hydrogen (approximately 4 wt.% in 200 s), which shows a better performance in the sorption kinetics of MgH$_2$–LiAlH$_4$ systems.

CHALLENGES AND POSSIBLE DEVELOPMENT STRATEGIES

Continuous plans to improve solid-state hydrogen storage materials will undoubtedly demonstrate a further positive effect on the development of hydrogen storage technologies and the widespread use of hydrogen in global energy transitions. Continuous research to identify new hydrogen storage materials indicates that the Mg–Li–Al system is a promising material for the future storage of hydrogen. Although the destabilized system of the Mg–Li–Al system has attracted a lot of attention and many types of research and development were carried out in this field, some problems and challenges still exist in achieving a suitable hydrogen storage material for practical applications. A few possible developmental strategies are listed as follows:

1) The addition of additives has shown considerable promise in improving the Mg–Li–Al system's performance. It is interesting to investigate the effect of other catalysts/additives to boost the performance of the Mg–Li–Al system and to understand the way catalysts/additives have an effect on improving the hydrogen storage properties of the Mg–Li–Al system.
2) The investigation on the reversible absorbs and desorbs hydrogen of the Mg–Li–Al system under moderate

TABLE 5 | Hydrogen storage performance of the Mg–Li–Al doped system with several additives compared with the undoped Mg–Li–Al system and unary MgH_2 and $LiAlH_4$.

System	Decomposition temperature (°C)	Desorption capacity (wt%)	Absorption capacity (wt%)	Absorption conditions (time and temperature)	Activation energy (kJ/mol)	Refs
As-received MgH_2	417	7.10	—	—	175.00	Sulaiman & Ismail, (2016)
As-milled MgH_2	345	6.80	4.10	60 min, 150°C	133.00	Sazelee et al. (2020a)
$MgH_2–K_2Ti_8O_{17}$	189	6.60	6.00	33 s, 200°C	116.30	Hu et al. (2021)
$MgH_2–TiO_2$	220	6.89	2.70	500 s, 100°C	76.10	Ma et al. (2020)
$MgH_2–K_2SiF_6$	282	~6.50	4.50	2 min, 250°C	114.00	Ismail et al. (2020)
$MgH_2–Ni_3Fe$	205	—	2.20	500 s, 100°C	82.10	Liu et al. (2020b)
$MgH_2–Ni@C$	230	6.80	5.60	350 s, 350°C	93.08	Meng et al. (2021)
$MgH_2–Na_3AlF_6$	290	6.50	—	—	129.00	Halim Yap et al. (2019)
$MgH_2–K_2ZrF_6$	250	~6.50	4.00	60 min, 300°C	80.00	Halim Yap et al. (2015)
As-received $LiAlH_4$	145, 175	7.40	—	—	—	Ali et al. (2019)
As-milled $LiAlH_4$	144, 174	7.40	—	—	80.00, 86.00	Ali et al. (2020)
$LiAlH_4–FeCl_2$	76	7.00	—	—	81.48, 105.10	Cai et al. (2016)
$LiAlH_4–SrTiO_3$	80, 120	6.50	—	—	70.00, 94.00	Ismail et al. (2021)
$LiAlH_4–LaFeO_3$	103, 153	6.40	—	—	73.00, 90.00	Sazelee et al. (2019)
$MgH_2–LiAlH_4$	135, 280	7.00	1.08	5 min, 300°C	125.60	Mustafa & Ismail, (2014)
$MgH_2–LiAlH_4–Fe_2O_3$	95, 270	7.00	2.78	5 min, 300°C	117.10	Mustafa & Ismail, (2014)
$MgH_2–LiAlH_4–MnFe_2O_4$	55, 170, 400	6.74	3.64	300 s, 300°C	55.80, 70.80, 96.50	Wan et al. (2013)
$MgH_2–LiAlH_4 –TiF_3$	70, 180	~7.00	3.30	5 min, 320°C	83.00	Ismail et al. (2011)
$MgH_2–LiAlH_4 –K_2TiF_6$	80, 250	~7.40	2.50	10 min, 300°C	107.00	Mustafa et al. (2015)
$MgH_2–LiAlH_4–Al_2TiO_5$	85, 230	7.10	1.90	25 min, 320°C	102.00	Sulaiman et al. (2021a)
$MgH_2–LiAlH_4–K_2ZrF_6$	95, 250	~7.00	3.30	20 min, 320°C	102.90	Halim Yap & Ismail, (2017)
$MgH_2–LiAlH_4–SrFe_{12}O_{19}$	80, 260	~7.10	5.10	60 min, 320°C	104.00	Sulaiman & Ismail, (2017)
$MgH_2–LiAlH_4–TiO_2$	70, 200	4.50	2.70	20 min, 320°C	102.50	Mustafa et al. (2021)

temperature and pressure must be the main target, and significant work is required to find the solution for the release and hydrogen uptake kinetics deteriorated during the cycling process.

3) It is reported that the formation of the Mg_2Al_3 during the rehydrogenation process has a negative effect on the hydrogen capacity and kinetic performance of the Mg–Li–Al system. The formation of Mg_2Al_3 could be avoided by applying a high pressure of hydrogen (> 10 MPa) during the rehydrogenation process. It is necessary to explore the ways of preventing the formation of Mg_2Al_3 without applying a high pressure of hydrogen, such as by using an appropriate additive or catalyst.

4) The hydrogen storage performance of the Mg–Li–Al system has been discovered to be influenced by the molar ratio and milling time. Furthermore, it is critical to investigate the other approaches, such as embedding materials in nanoconfinement, which could improve the hydrogen storage properties of the Mg–Li–Al system.

Therefore, we believe that with continuous effort, the limitations on the development of the Mg–Li–Al system as an ideal hydrogen storage material might be overcome and that the Mg–Li–Al system

with favorable kinetics and thermodynamics should be one of the near-term goals.

CONCLUSION

In this review, it was clear that the transition from the current energy economy to cleaner energy like hydrogen was motivated by environmental and economic factors. Possible current approaches to store hydrogen are in the liquid state, compressed gas state, and solid state. However, due to the large amount of hydrogen that can be stored in a small amount and safety considerations, solid-state hydrogen storage systems are attractive to research. This comprehensive review highlighted the higher desorption temperature and sluggish sorption kinetics in MgH_2, which can be overcome through the destabilization concept (addition of $LiAlH_4$). Many researchers explored the reaction between the Mg–Li–Al system, including the ratio, the milling time, and the addition of an additive/catalyst to this composite. Interestingly, the doping Mg–Li–Al system with the catalyst can reduce the onset desorption temperature to below 60°C. The intermediate forms of $Li_{0.92}Mg_{4.08}$ and $Mg_{17}Al_{12}$ were eventually formed in the

Mg–Li–Al composites. Cycling measurements show that $Li_{0.92}Mg_{4.08}$ and $Mg_{17}Al_{12}$ are fully reversible absorbs and desorbs of hydrogen. However, the Mg–Li–Al composites are still in their early development and need more time to prove themselves as viable long-term solutions for solid-state hydrogen storage. Further study, such as on doping with other additives/catalysts, could investigate the different milling times and ratios that should be focused on for the further design of advanced solid-state hydrogen storage materials.

AUTHOR CONTRIBUTIONS

All authors listed have made a substantial, direct, and intellectual contribution to the work and approved it for publication.

REFERENCES

Abdin, Z., Zafaranloo, A., Rafiee, A., Mérida, W., Lipiński, W., and Khalilpour, K. R. (2020). Hydrogen as an Energy Vector. *Renew. Sust. Energ. Rev.* 120, 109620. doi:10.1016/j.rser.2019.109620

Ali, N. A., Idris, N. H., Sazelee, N. A., Yahya, M. S., Yap, F. A. H., and Ismail, M. (2019). Catalytic Effects of MgFe2O4 Addition on the Dehydrogenation Properties of LiAlH4. *Int. J. Hydrogen Energ.* 44 (52), 28227–28234. doi:10.1016/j.ijhydene.2019.09.083

Ali, N. A., and Ismail, M. (2021). Advanced Hydrogen Storage of the Mg-Na-Al System: A Review. *J. Magnesium Alloys* 9 (4), 1111–1122. doi:10.1016/j.jma.2021.03.031

Ali, N. A., Sazelee, N. A., and Ismail, M. (2021). An Overview of Reactive Hydride Composite (RHC) for Solid-State Hydrogen Storage Materials. *Int. J. Hydrogen Energ.* 46 (62), 31674–31698. doi:10.1016/j.ijhydene.2021.07.058

Ali, N. A., Sazelee, N., Yahya, M. S., and Ismail, M. (2020). Influence of K2NbF7 Catalyst on the Desorption Behavior of LiAlH4. *Front. Chem.* 8 (457), 457. doi:10.3389/fchem.2020.00457

Baricco, M., Rahman, M. W., Livraghi, S., Castellero, A., Enzo, S., and Giamello, E. (2012). Effects of BaRuO3 Addition on Hydrogen Desorption in MgH2. *J. Alloys Comp.* 536, S216–S221. doi:10.1016/j.jallcom.2011.12.008

Barkhordarian, G., Klassen, T., Dornheim, M., and Bormann, R. (2007). Unexpected Kinetic Effect of MgB2 in Reactive Hydride Composites Containing Complex Borohydrides. *J. Alloys Comp.* 440 (1), L18–L21. doi:10.1016/j.jallcom.2006.09.048

Bendyna, J. K., Dyjak, S., and Notten, P. H. L. (2015). The Influence of ball-milling Time on the Dehydrogenation Properties of the NaAlH4-MgH2 Composite. *Int. J. Hydrogen Energ.* 40 (11), 4200–4206. doi:10.1016/j.ijhydene.2015.01.026

Cai, J., Zang, L., Zhao, L., Liu, J., and Wang, Y. (2016). Dehydrogenation Characteristics of LiAlH 4 Improved by *In-Situ* Formed Catalysts. *J. Energ. Chem.* 25 (5), 868–873. doi:10.1016/j.jechem.2016.06.004

Chen, R., Wang, X., Xu, L., Chen, L., Li, S., and Chen, C. (2010). An Investigation on the Reaction Mechanism of LiAlH4-MgH2 Hydrogen Storage System. *Mater. Chem. Phys.* 124 (1), 83–87. doi:10.1016/j.matchemphys.2010.05.070

Correa-Jullian, C., and Groth, K. M. (2022). Data Requirements for Improving the Quantitative Risk Assessment of Liquid Hydrogen Storage Systems. *Int. J. Hydrogen Energ.* 47 (6), 4222–4235. doi:10.1016/j.ijhydene.2021.10.266

Crivello, J.-C., Denys, R. V., Dornheim, M., Felderhoff, M., Grant, D. M., Huot, J., et al. (2016). Mg-based Compounds for Hydrogen and Energy Storage. *Appl. Phys. A.* 122 (2), 85. doi:10.1007/s00339-016-9601-1

Czujko, T., Zaranski, Z., Malka, I. E., and Wronski, Z. (2011). Composite Behaviour of MgH2 and Complex Hydride Mixtures Synthesized by ball Milling. *J. Alloys Comp.* 509, S604–S607. doi:10.1016/j.jallcom.2010.08.133

Daulbayev, C., Lesbayev, B., Bakbolat, B., Kaidar, B., Sultanov, F., Yeleuov, M., et al. (2022). A Mini-Review on Recent Trends in Prospective Use of Porous 1D Nanomaterials for Hydrogen Storage. *South Afr. J. Chem. Eng.* 39, 52–61. doi:10.1016/j.sajce.2021.11.008

FUNDING

ACKNOWLEDGMENTS

David, E. (2005). An Overview of Advanced Materials for Hydrogen Storage. *J. Mater. Process. Tech.* 162-163, 169–177. doi:10.1016/j.jmatprotec.2005.02.027

Dematteis, E. M., Cuevas, F., and Latroche, M. (2021). Hydrogen Storage Properties of Mn and Cu for Fe Substitution in TiFe0.9 Intermetallic Compound. *J. Alloys Comp.* 851, 156075. doi:10.1016/j.jallcom.2020.156075

Ding, X., Zhu, Y., Wei, L., Li, Y., and Li, L. (2013). Synergistic Hydrogen Desorption of HCS MgH2 + LiAlH4 Composite. *Energy* 55, 933–938. doi:10.1016/j.energy.2013.04.043

Doğan, M., Sabaz, P., Bïcîl, Z., Koçer Kizilduman, B., and Turhan, Y. (2020). Activated Carbon Synthesis from Tangerine Peel and its Use in Hydrogen Storage. *J. Energ. Inst.* 93 (6), 2176–2185. doi:10.1016/j.joei.2020.05.011

Dornheim, M., Doppiu, S., Barkhordarian, G., Boesenberg, U., Klassen, T., Gutfleisch, O., et al. (2007). Hydrogen Storage in Magnesium-Based Hydrides and Hydride Composites. *Scripta Materialia* 56 (10), 841–846. doi:10.1016/j.scriptamat.2007.01.003

Dunn, S. (2002). Hydrogen Futures: toward a Sustainable Energy System. *Int. J. Hydrogen Energ.* 27 (3), 235–264. doi:10.1016/S0360-3199(01)00131-8

Eftekhari, A., and Fang, B. (2017). Electrochemical Hydrogen Storage: Opportunities for Fuel Storage, Batteries, Fuel Cells, and Supercapacitors. *Int. J. Hydrogen Energ.* 42 (40), 25143–25165. doi:10.1016/j.ijhydene.2017.08.103

El Khatabi, M., Naji, S., Bhihi, M., Benyoussef, A., El Kenz, A., and Loulidi, M. (2018). Effects of Double Substitution on MgH2 Hydrogen Storage Properties: An Ab Initio Study. *J. Alloys Comp.* 743, 666–671. doi:10.1016/j.jallcom.2017.11.083

Graetz, J., Wegrzyn, J., and Reilly, J. J. (2008). Regeneration of Lithium Aluminum Hydride. *J. Am. Chem. Soc.* 130 (52), 17790–17794. doi:10.1021/ja805353w

Halim Yap, F. A., Mustafa, N. S., and Ismail, M. (2015). A Study on the Effects of K2ZrF6 as an Additive on the Microstructure and Hydrogen Storage Properties of MgH2. *RSC Adv.* 5 (12), 9255–9260. doi:10.1039/C4RA12487A

Halim Yap, F. A., Sulaiman, N. N., and Ismail, M. (2019). Understanding the Dehydrogenation Properties of MgH2 Catalysed by Na3AlF6. *Int. J. Hydrogen Energ.* 44 (58), 30583–30590. doi:10.1016/j.ijhydene.2018.02.073

Hsu, W.-C., Yang, C.-H., Tan, C.-Y., and Tsai, W.-T. (2014b). *In Situ* synchrotron X-ray Diffraction Study on the Dehydrogenation Behavior of LiAlH4-MgH2 Composites. *J. Alloys Comp.* 599 (0), 164–169. doi:10.1016/j.jallcom.2014.02.064

Hsu, W.-C., Yang, C.-H., and Tsai, W.-T. (2014a). Catalytic Effect of MWCNTs on the Dehydrogenation Behavior of LiAlH4. *Int. J. Hydrogen Energ.* 39 (2), 927–933. doi:10.1016/j.ijhydene.2013.10.155

Hu, S., Zhang, H., Yuan, Z., Wang, Y., Fan, G., Fan, Y., et al. (2021). Ultrathin K2Ti8O17 Nanobelts for Improving the Hydrogen Storage Kinetics of MgH2. *J. Alloys Comp.* 881, 160571. doi:10.1016/j.jallcom.2021.160571

Imamura, H., Masanari, K., Kusuhara, M., Katsumoto, H., Sumi, T., and Sakata, Y. (2005). High Hydrogen Storage Capacity of Nanosized Magnesium Synthesized by High Energy ball-milling. *J. Alloys Comp.* 386 (1), 211–216. doi:10.1016/j.jallcom.2004.04.145

Ismail, M. (2021). Effect of Adding Different Percentages of HfCl4 on the Hydrogen Storage Properties of MgH2. *Int. J. Hydrogen Energ.* 46 (12), 8621–8628. doi:10.1016/j.ijhydene.2020.12.068

Ismail, M. (2015). Effect of LaCl 3 Addition on the Hydrogen Storage Properties of MgH 2. *Energy* 79, 177–182. doi:10.1016/j.energy.2014.11.001

Ismail, M., and Mustafa, N. S. (2016). Improved Hydrogen Storage Properties of NaAlH4MgH2LiBH4 Ternary-Hydride System Catalyzed by TiF3. *Int. J. Hydrogen Energ.* 41 (40), 18107–18113. doi:10.1016/j.ijhydene.2016.07.090

Ismail, M., Sazelee, N. A., Ali, N. A., and Suwarno, S. (2021). Catalytic Effect of SrTiO3 on the Dehydrogenation Properties of LiAlH4. *J. Alloys Comp.* 855, 157475. doi:10.1016/j.jallcom.2020.157475

Ismail, M. (2016). The Hydrogen Storage Properties of Destabilized MgH2-AlH3 (2:1) System. *Mater. Today Proc.* 3 (Suppl. 1), S80–S87. doi:10.1016/j.matpr.2016.01.011

Ismail, M., Yahya, M. S., Sazelee, N. A., Ali, N. A., Yap, F. A. H., and Mustafa, N. S. (2020). The Effect of K2SiF6 on the MgH2 Hydrogen Storage Properties. *J. Magnesium Alloys* 8 (3), 832–840. doi:10.1016/j.jma.2020.04.002

Ismail, M., Yap, F. A. H., Sulaiman, N. N., and Ishak, M. H. I. (2016). Hydrogen Storage Properties of a Destabilized MgH2Sn System with TiF3 Addition. *J. Alloys Comp.* 678, 297–303. doi:10.1016/j.jallcom.2016.03.168

Ismail, M., Zhao, Y., and Dou, S. X. (2013). An Investigation on the Hydrogen Storage Properties and Reaction Mechanism of the Destabilized MgH2-Na3AlH6 (4:1) System. *Int. J. Hydrogen Energ.* 38 (3), 1478–1483. doi:10.1016/j.ijhydene.2012.11.035

Ismail, M., Zhao, Y., Yu, X. B., and Dou, S. X. (2011). Effect of Different Additives on the Hydrogen Storage Properties of the MgH2-LiAlH4 Destabilized System. *RSC Adv.* 1 (3), 408–414. doi:10.1039/C1RA00209K

Jain, I. P., Lal, C., and Jain, A. (2010). Hydrogen Storage in Mg: A Most Promising Material. *Int. J. Hydrogen Energ.* 35 (10), 5133–5144. doi:10.1016/j.ijhydene.2009.08.088

Jang, J.-W., Shim, J.-H., Cho, Y. W., and Lee, B.-J. (2006). Thermodynamic Calculation of LiH↔Li3AlH6↔LiAlH4 Reactions. *J. Alloys Comp.* 420 (1), 286–290. doi:10.1016/j.jallcom.2005.10.040

Jangir, M., Jain, A., Agarwal, S., Zhang, T., Kumar, S., Selvaraj, S., et al. (2018). The enhanced de/re-hydrogenation performance of MgH2 with TiH2 additive. *Int. J. Energ. Res* 42 (3), 1139–1147. doi:10.1002/er.3911

Jiang, W., Sun, P., Li, P., Zuo, Z., and Huang, Y. (2021). Transient thermal Behavior of Multi-Layer Insulation Coupled with Vapor Cooled Shield Used for Liquid Hydrogen Storage Tank. *Energy* 231, 120859. doi:10.1016/j.energy.2021.120859

Kato, S., Borgschulte, A., Bielmann, M., and Züttel, A. (2012). Interface Reactions and Stability of a Hydride Composite (NaBH4 + MgH2). *Phys. Chem. Chem. Phys.* 14 (23), 8360–8368. doi:10.1039/C2CP23491B

Ke, X., and Chen, C. (2007). Thermodynamic Functions and Pressure-Temperature Phase Diagram of Lithium Alanates Byab Initiocalculations. *Phys. Rev. B* 76 (2), 024112. doi:10.1103/PhysRevB.76.024112

Khurana, T., Prasad, B., Ramamurthi, K., and Murthy, S. (2006). Thermal Stratification in Ribbed Liquid Hydrogen Storage Tanks. *Int. J. Hydrogen Energ.* 31 (15), 2299–2309. doi:10.1016/j.ijhydene.2006.02.032

Kojima, Y. (2019). Hydrogen Storage Materials for Hydrogen and Energy Carriers. *Int. J. Hydrogen Energ.* 44 (33), 18179–18192. doi:10.1016/j.ijhydene.2019.05.119

Léon, A., Zabara, O., Sartori, S., Eigen, N., Dornheim, M., Klassen, T., et al. (2009). Investigation of (Mg, Al, Li, H)-based Hydride and Alanate Mixtures Produced by Reactive ball Milling. *J. Alloys Comp.* 476 (1-2), 425–428. doi:10.1016/j.jallcom.2008.09.023

Li, X., Qin, Y., Fu, J., and Zhao, J. (2015). A Gupta Potential for Magnesium in Hcp Phase. *Comput. Mater. Sci.* 98, 328–332. doi:10.1016/j.commatsci.2014.11.023

Li, Z., Wang, H., Ouyang, L., Liu, J., and Zhu, M. (2019). Achieving superior De-/hydrogenation Properties of C15 Laves Phase Y-Fe-Al Alloys by A-Side Substitution. *J. Alloys Comp.* 787, 158–164. doi:10.1016/j.jallcom.2019.02.074

Liang, Z., Yao, Z., Xiao, X., Kou, H., Luo, W., Chen, C., et al. (2020). The Functioning Mechanism of Al Valid Substitution for Co in Improving the Cycling Performance of Zr-Co-Al Based Hydrogen Isotope Storage Alloys. *J. Alloys Comp.* 848, 156618. doi:10.1016/j.jallcom.2020.156618

Lin, H.-J., Matsuda, J., Li, H.-W., Zhu, M., and Akiba, E. (2015). Enhanced Hydrogen Desorption Property of MgH2 with the Addition of Cerium Fluorides. *J. Alloys Comp.* 645, S392–S396. doi:10.1016/j.jallcom.2014.12.102

Lin, I.-C., and Tsai, W.-T. (2017). "*In Situ* synchrotron X-ray Diffraction Study on the Rehydrogenation Behavior of MgH2-LiAlH4 Composites," *in SituSynchrotron X-ray Diffraction Study on the Rehydrogenation Behavior of MgH₂-LiAlH₄ Composites.* Sapporo, Japan: International Conference on Applied System Innovation, 1918–1921. doi:10.1109/ICASI.2017.7988326

Liu, C., Guo, P., Qiao, Y., and Zhang, S. (2020a). A First-Principle Study on the Formation and Migration of AlH3 Defect on (1 1 2) NaAlH4 Surface. *Chem. Phys.* 538, 110871. doi:10.1016/j.chemphys.2020.110871

Liu, H., Lu, C., Wang, X., Xu, L., Huang, X., Wang, X., et al. (2021). Combinations of V2C and Ti3C2 MXenes for Boosting the Hydrogen Storage Performances of MgH2. *ACS Appl. Mater. Inter.* 13 (11), 13235–13247. doi:10.1021/acsami.0c23150

Liu, H., Wang, X., Liu, Y., Dong, Z., Cao, G., Li, S., et al. (2013). Improved hydrogen storage properties of MgH2 by ball milling with AlH3: preparations, de/rehydriding properties, and reaction mechanisms. *J. Mater. Chem. A.* 1 (40), 12527–12535. doi:10.1039/c3ta11953j

Liu, H., Wang, X., Liu, Y., Dong, Z., Ge, H., Li, S., et al. (2014). Hydrogen Desorption Properties of the MgH2-AlH3 Composites. *J. Phys. Chem. C* 118 (1), 37–45. doi:10.1021/jp407018w

Liu, J., Ma, Z., Liu, Z., Tang, Q., Zhu, Y., Lin, H., et al. (2020b). Synergistic Effect of rGO Supported Ni3Fe on Hydrogen Storage Performance of MgH2. *Int. J. Hydrogen Energ.* 45 (33), 16622–16633. doi:10.1016/j.ijhydene.2020.04.104

Lu, X., Zhang, L., Yu, H., Lu, Z., He, J., Zheng, J., et al. (2021). Achieving superior Hydrogen Storage Properties of MgH2 by the Effect of TiFe and Carbon Nanotubes. *Chem. Eng. J.* 422, 130101. doi:10.1016/j.cej.2021.130101

Luo, Q., Li, J., Li, B., Liu, B., Shao, H., and Li, Q. (2019). Kinetics in Mg-Based Hydrogen Storage Materials: Enhancement and Mechanism. *J. Magnesium Alloys* 7 (1), 58–71. doi:10.1016/j.jma.2018.12.001

Ma, Z., Liu, J., Zhu, Y., Zhao, Y., Lin, H., Zhang, Y., et al. (2020). Crystal-facet-dependent Catalysis of Anatase TiO2 on Hydrogen Storage of MgH2. *J. Alloys Comp.* 822, 153553. doi:10.1016/j.jallcom.2019.153553

Ma, Z., Panda, S., Zhang, Q., Sun, F., Khan, D., Ding, W., et al. (2021). Improving Hydrogen Sorption Performances of MgH2 through Nanoconfinement in a Mesoporous CoS Nano-Boxes Scaffold. *Chem. Eng. J.* 406, 126790. doi:10.1016/j.cej.2020.126790

Mao, J. F., Yu, X. B., Guo, Z. P., Liu, H. K., Wu, Z., and Ni, J. (2009). Enhanced Hydrogen Storage Performances of NaBH4-MgH2 System. *J. Alloys Comp.* 479 (1-2), 619–623. doi:10.1016/j.jallcom.2009.01.012

Mao, J., Guo, Z., Yu, X., Ismail, M., and Liu, H. (2011). Enhanced Hydrogen Storage Performance of LiAlH4-MgH2-TiF3 Composite. *Int. J. Hydrogen Energ.* 36 (9), 5369–5374. doi:10.1016/j.ijhydene.2011.02.001

Marques, F., Pinto, H. C., Figueroa, S. J. A., Winkelmann, F., Felderhoff, M., Botta, W. J., et al. (2020). Mg-containing Multi-Principal Element Alloys for Hydrogen Storage: A Study of the MgTiNbCr0.5Mn0.5Ni0.5 and Mg0.68TiNbNi0.55 Compositions. *Int. J. Hydrogen Energ.* 45 (38), 19539–19552. doi:10.1016/j.ijhydene.2020.05.069

Meng, Q., Huang, Y., Ye, J., Xia, G., Wang, G., Dong, L., et al. (2021). Electrospun Carbon Nanofibers with *In-Situ* Encapsulated Ni Nanoparticles as Catalyst for Enhanced Hydrogen Storage of MgH2. *J. Alloys Comp.* 851, 156874. doi:10.1016/j.jallcom.2020.156874

Milanović, I., Milošević, S., Matović, L., Vujasin, R., Novaković, N., Checchetto, R., et al. (2013). Hydrogen Desorption Properties of MgH2/LiAlH4 Composites. *Int. J. Hydrogen Energ.* 38 (27), 12152–12158. doi:10.1016/j.ijhydene.2013.05.020

Montone, A., Aurora, A., Mirabile Gattia, D., and Vittori Antisari, M. (2010). On the Barriers Limiting the Reaction Kinetics between Catalysed Mg and Hydrogen. *Scripta Materialia* 63 (4), 456–459. doi:10.1016/j.scriptamat.2010.05.003

Mulas, G., Campesi, R., Garroni, S., Napolitano, E., Milanese, C., Dolci, F., et al. (2012). Hydrogen Storage in 2NaBH4+MgH2 Mixtures: Destabilization by Additives and Nanoconfinement. *J. Alloys Comp.* 536, S236–S240. doi:10.1016/j.jallcom.2011.12.042

Mustafa, N. S., Idris, N. H., and Ismail, M. (2015). Effect of K 2 TiF 6 Additive on the Hydrogen Storage Properties of 4MgH 2 -LiAlH 4 Destabilized System. *Int. J. Hydrogen Energ.* 40 (24), 7671–7677. doi:10.1016/j.ijhydene.2014.10.112

Mustafa, N. S., and Ismail, M. (2014). Enhanced Hydrogen Storage Properties of 4MgH2 + LiAlH4 Composite System by Doping with Fe2O3 Nanopowder. *Int. J. Hydrogen Energ.* 39 (0), 7834–7841. doi:10.1016/j.ijhydene.2014.02.118

Mustafa, N. S., Yahya, M. S., Itam Sulaiman, N. N., Abdul Halim Yap, M. F. A., and Ismail, M. (2021). Enhanced the Hydrogen Storage Properties and Reaction Mechanisms of 4MgH 2 + LiAlH 4 Composite System by Addition with TiO 2. *Int. J. Energ. Res* 45 (15), 21365–21374. doi:10.1002/er.7187

Niaz, S., Manzoor, T., and Pandith, A. H. (2015). Hydrogen Storage: Materials, Methods and Perspectives. *Renew. Sust. Energ. Rev.* 50, 457–469. doi:10.1016/j.rser.2015.05.011

Ouyang, L., Liu, F., Wang, H., Liu, J., Yang, X.-S., Sun, L., et al. (2020). Magnesium-based Hydrogen Storage Compounds: A Review. *J. Alloys Comp.* 832, 154865. doi:10.1016/j.jallcom.2020.154865

Peláez-Peláez, S., Colmenar-Santos, A., Pérez-Molina, C., Rosales, A.-E., and Rosales-Asensio, E. (2021). Techno-economic Analysis of a Heat and Power Combination System Based on Hybrid Photovoltaic-Fuel Cell Systems Using Hydrogen as an Energy Vector. *Energy* 224, 120110. doi:10.1016/j.energy.2021.120110

Polanski, M., Bystrzycki, J., Varin, R. A., Plocinski, T., and Pisarek, M. (2011). The Effect of Chromium (III) Oxide (Cr2O3) Nanopowder on the Microstructure and Cyclic Hydrogen Storage Behavior of Magnesium Hydride (MgH2). *J. Alloys Comp.* 509 (5), 2386–2391. doi:10.1016/j.jallcom.2010.11.026

Rafi-ud-din, Xuanhui, Q., Zahid, G. H., Asghar, Z., Shahzad, M., Iqbal, M., et al. (2014). Improved Hydrogen Storage Performances of MgH2-NaAlH4 System Catalyzed by TiO2 Nanoparticles. *J. Alloys Comp.* 604, 317–324. doi:10.1016/j.jallcom.2014.03.150

Ranjbar, A., Guo, Z. P., Yu, X. B., Wexler, D., Calka, A., Kim, C. J., et al. (2009). Hydrogen Storage Properties of MgH2-SiC Composites. *Mater. Chem. Phys.* 114 (1), 168–172. doi:10.1016/j.matchemphys.2008.09.001

Ranjbar, A., Ismail, M., Guo, Z. P., Yu, X. B., and Liu, H. K. (2010). Effects of CNTs on the Hydrogen Storage Properties of MgH2 and MgH2-BCC Composite. *Int. J. Hydrogen Energ.* 35 (15), 7821–7826. doi:10.1016/j.ijhydene.2010.05.080

Reilly, J. J., and Wiswall, R. H. (1968). Reaction of Hydrogen with Alloys of Magnesium and Nickel and the Formation of Mg2NiH4. *Inorg. Chem.* 7 (11), 2254–2256. doi:10.1021/ic50069a016

Sabitu, S. T., and Goudy, A. J. (2012). Dehydrogenation Kinetics and Modeling Studies of MgH2 Enhanced by Transition Metal Oxide Catalysts Using Constant Pressure Thermodynamic Driving Forces. *Metals* 2 (3), 219–228. doi:10.3390/met2030219

Sadhasivam, T., Kim, H.-T., Jung, S., Roh, S.-H., Park, J.-H., and Jung, H.-Y. (2017). Dimensional Effects of Nanostructured Mg/MgH 2 for Hydrogen Storage Applications: A Review. *Renew. Sust. Energ. Rev.* 72, 523–534. doi:10.1016/j.rser.2017.01.107

Sakintuna, B., Lamaridarkrim, F., and Hirscher, M. (2007). Metal Hydride Materials for Solid Hydrogen Storage: A Review☆. *Int. J. Hydrogen Energ.* 32 (9), 1121–1140. doi:10.1016/j.ijhydene.2006.11.022

Sartbaeva, A., Kuznetsov, V. L., Wells, S. A., and Edwards, P. P. (2008). Hydrogen Nexus in a Sustainable Energy Future. *Energy Environ. Sci.* 1 (1), 79–85. doi:10.1039/B810104N

Satyapal, S., Petrovic, J., Read, C., Thomas, G., and Ordaz, G. (2007). The U.S. Department of Energy's National Hydrogen Storage Project: Progress towards Meeting Hydrogen-Powered Vehicle Requirements. *Catal. Today* 120 (3), 246–256. doi:10.1016/j.cattod.2006.09.022

Sazelee, N. A., Idris, N. H., Md Din, M. F., Mustafa, N. S., Ali, N. A., Yahya, M. S., et al. (2018). Synthesis of BaFe12O19 by Solid State Method and its Effect on Hydrogen Storage Properties of MgH2. *Int. J. Hydrogen Energ.* 43 (45), 20853–20860. doi:10.1016/j.ijhydene.2018.09.125

Sazelee, N. A., Idris, N. H., Md Din, M. F., S.Yahya, M., Ali, N. A., and Ismail, M. (2020a). LaFeO3 Synthesised by Solid-State Method for Enhanced Sorption Properties of MgH2. *Results Phys.* 16, 102844. doi:10.1016/j.rinp.2019.102844

Sazelee, N. A., and Ismail, M. (2021). Recent Advances in Catalyst-Enhanced LiAlH4 for Solid-State Hydrogen Storage: A Review. *Int. J. Hydrogen Energ.* 46 (13), 9123–9141. doi:10.1016/j.ijhydene.2020.12.208

Sazelee, N. A., Yahya, M. S., Ali, N. A., Idris, N. H., and Ismail, M. (2020b). Enhancement of Dehydrogenation Properties in LiAlH4 Catalysed by BaFe12O19. *J. Alloys Comp.* 835, 155183. doi:10.1016/j.jallcom.2020.155183

Sazelee, N. A., Yahya, M. S., Idris, N. H., Md Din, M. F., and Ismail, M. (2019). Desorption Properties of LiAlH4 Doped with LaFeO3 Catalyst. *Int. J. Hydrogen Energ.* 44 (23), 11953–11960. doi:10.1016/j.ijhydene.2019.03.102

Schlapbach, L., Shaltiel, D., and Oelhafen, P. (1979). Catalytic Effect in the Hydrogenation of Mg and Mg Compounds: Surface Analysis of MgMg2Ni

and Mg2Ni. *Mater. Res. Bull.* 14 (9), 1235–1246. doi:10.1016/0025-5408(79)90220-4

Sulaiman, N. N., and Ismail, M. (2016). Enhanced Hydrogen Storage Properties of MgH2 Co-catalyzed with K2NiF6 and CNTs. *Dalton Trans.* 45 (48), 19380–19388. doi:10.1039/C6DT03646E

Sulaiman, N. N., Ismail, M., Rashid, A. H. A., Ali, N. A., Sazelee, N. A., and Timmiati, S. N. (2021a). Hydrogen Storage Properties of Mg-Li-Al Composite System Doped with Al2TiO5 Catalyst for Solid-State Hydrogen Storage. *J. Alloys Comp.* 870, 159469. doi:10.1016/j.jallcom.2021.159469

Sulaiman, N. N., and Ismail, M. (2017). Study the Effect of SrFe12O19 on MgH2/LiAlH4 Composite for Solid-State Hydrogen Storage. *Int. J. Hydrogen Energ.* 42 (50), 29830–29839. doi:10.1016/j.ijhydene.2017.10.071

Sulaiman, N. N., Ismail, M., Timmiati, S. N., and Lim, K. L. (2021b). Improved Hydrogen Storage Performances of LiAlH 4 + Mg(BH 4) 2 Composite with TiF 3 Addition. *Int. J. Energ. Res* 45 (2), 2882–2898. doi:10.1002/er.5984

Thapa, B. S., Neupane, B., Yang, H.-s., and Lee, Y.-H. (2021). Green Hydrogen Potentials from Surplus Hydro Energy in Nepal. *Int. J. Hydrogen Energ.* 46 (43), 22256–22267. doi:10.1016/j.ijhydene.2021.04.096

Urgnani, J., Torres, F. J., Palumbo, M., and Baricco, M. (2008). Hydrogen Release from Solid State NaBH4. *Int. J. Hydrogen Energ.* 33 (12), 3111–3115. doi:10.1016/j.ijhydene.2008.03.031

Vajo, J. J., Mertens, F., Ahn, C. C., Bowman, R. C., and Fultz, B. (2004). Altering Hydrogen Storage Properties by Hydride Destabilization through Alloy Formation: LiH and MgH2 Destabilized with Si. *J. Phys. Chem. B* 108 (37), 13977–13983. doi:10.1021/jp040060h

Vajo, J. J., and Olson, G. L. (2007). Hydrogen Storage in Destabilized Chemical Systems. *Scripta Materialia* 56 (10), 829–834. doi:10.1016/j.scriptamat.2007.01.002

Vajo, J. J., Salguero, T. T., Gross, A. F., Skeith, S. L., and Olson, G. L. (2007). Thermodynamic Destabilization and Reaction Kinetics in Light Metal Hydride Systems. *J. Alloys Comp.* 446-447 (0), 409–414. doi:10.1016/j.jallcom.2007.02.080

Vittetoe, A. W., Niemann, M. U., Srinivasan, S. S., McGrath, K., Kumar, A., Goswami, D. Y., et al. (2009). Destabilization of LiAlH4 by Nanocrystalline MgH2. *Int. J. Hydrogen Energ.* 34 (5), 2333–2339. doi:10.1016/j.ijhydene.2009.01.025

Wan, Q., Li, P., Li, Z., Zhai, F., Qu, X., and Volinsky, A. A. (2013). Improved Hydrogen Storage Performance of MgH2-LiAlH4 Composite by Addition of MnFe2O4. *J. Phys. Chem. C* 117 (51), 26940–26947. doi:10.1021/jp410449q

Wang, Y., Wang, Y., Wang, X., Zhang, H., Jiao, L., and Yuan, H. (2014). Destabilization Effects of Mg(AlH 4) 2 on MgH 2 : Improved Desorption Performances and its Reaction Mechanism. *Int. J. Hydrogen Energ.* 39 (31), 17747–17753. doi:10.1016/j.ijhydene.2014.08.117

Xia, Y., Wei, S., Huang, Q., Li, J., Cen, X., Zhang, H., et al. (2020). Facile Synthesis of NiCo2O4-Anchored Reduced Graphene Oxide Nanocomposites as Efficient Additives for Improving the Dehydrogenation Behavior of Lithium Alanate. *Inorg. Chem. Front.* 7 (5), 1257–1272. doi:10.1039/C9QI01451A

Yang, L., Yu, L. L., Wei, H. W., Li, W. Q., Zhou, X., and Tian, W. Q. (2019). Hydrogen Storage of Dual-Ti-Doped Single-Walled Carbon Nanotubes. *Int. J. Hydrogen Energ.* 44 (5), 2960–2975. doi:10.1016/j.ijhydene.2018.12.028

Yang, Y., Xiong, X., Chen, J., Peng, X., Chen, D., and Pan, F. (2021). Research Advances in Magnesium and Magnesium Alloys Worldwide in 2020. *J. Magnesium Alloys* 9 (3), 705–747. doi:10.1016/j.jma.2021.04.001

Yao, L., Lyu, X., Zhang, J., Liu, Y., Zhu, Y., Lin, H., et al. (2020a). Remarkable Synergistic Effects of Mg2NiH4 and Transition Metal Carbides (TiC, ZrC, WC) on Enhancing the Hydrogen Storage Properties of MgH2. *Int. J. Hydrogen Energ.* 45 (11), 6765–6779. doi:10.1016/j.ijhydene.2019.12.139

Yao, P., Jiang, Y., Liu, Y., Wu, C., Chou, K.-C., Lyu, T., et al. (2020b). Catalytic Effect of Ni@rGO on the Hydrogen Storage Properties of MgH2. *J. Magnesium Alloys* 8 (2), 461–471. doi:10.1016/j.jma.2019.06.006

Yap, F. A. H., and Ismail, M. (2017). The Hydrogen Storage Properties of Mg-Li-Al Composite System Catalyzed by K 2 ZrF 6. *J. Phys. Chem. Sol.* 104, 214–220. doi:10.1016/j.jpcs.2017.01.021

Ye, Y., Lu, J., Ding, J., Wang, W., and Yan, J. (2020). Numerical Simulation on the Storage Performance of a Phase Change Materials Based Metal Hydride Hydrogen Storage Tank. *Appl. Energ.* 278, 115682. doi:10.1016/j.apenergy.2020.115682

Yu, X., Tang, Z., Sun, D., Ouyang, L., and Zhu, M. (2017). Recent Advances and Remaining Challenges of Nanostructured Materials for Hydrogen Storage Applications. *Prog. Mater. Sci.* 88, 1–48. doi:10.1016/j.pmatsci.2017.03.001

Zacharia, R., and Rather, S. U. (20152015). Review of Solid State Hydrogen Storage Methods Adopting Different Kinds of Novel Materials. *J. Nanomater.* 2015, 1–18. doi:10.1155/2015/914845

Zaluska, A., Zaluski, L., and Ström Olsen, J. O. (1999). Nanocrystalline Magnesium for Hydrogen Storage. *J. Alloys Comp.* 288 (1), 217–225. doi:10.1016/S0925-8388(99)00073-0

Zhai, F., Li, P., Sun, A., Wu, S., Wan, Q., Zhang, W., et al. (2012). Significantly Improved Dehydrogenation of LiAlH4 Destabilized by MnFe2O4 Nanoparticles. *J. Phys. Chem. C* 116 (22), 11939–11945. doi:10.1021/jp302721w

Zhang, J., Li, Z., Wu, Y., Guo, X., Ye, J., Yuan, B., et al. (2019a). Recent Advances on the thermal Destabilization of Mg-Based Hydrogen Storage Materials. *RSC Adv* 9(1), 408–428. doi:10.1039/C8RA05596C

Zhang, J., Shan, J., Li, P., Zhai, F., Wan, Q., Liu, Z., et al. (2015). Dehydrogenation Mechanism of ball-milled MgH 2 Doped with Ferrites (CoFe 2 O 4 , ZnFe 2 O 4 , MnFe 2 O 4 and Mn 0.5 Zn 0.5 Fe 2 O 4) Nanoparticles. *J. Alloys Comp.* 643, 174–180. doi:10.1016/j.jallcom.2015.04.135

Zhang, J., Yan, S., Xia, G., Zhou, X., Lu, X., Yu, L., et al. (2021). Stabilization of Low-Valence Transition Metal towards Advanced Catalytic Effects on the Hydrogen Storage Performance of Magnesium Hydride. *J. Magnesium Alloys* 9 (2), 647–657. doi:10.1016/j.jma.2020.02.029

Zhang, J., Zhu, Y., Yao, L., Xu, C., Liu, Y., and Li, L. (2019b). State of the Art Multi-Strategy Improvement of Mg-Based Hydrides for Hydrogen Storage. *J. Alloys Comp.* 782, 796–823. doi:10.1016/j.jallcom.2018.12.217

Zhang, T., Isobe, S., Jain, A., Wang, Y., Yamaguchi, S., Miyaoka, H., et al. (2017). Enhancement of Hydrogen Desorption Kinetics in Magnesium Hydride by Doping with Lithium Metatitanate. *J. Alloys Comp.* 711, 400–405. doi:10.1016/j.jallcom.2017.03.361

Zhang, Y., Tian, Q.-F., Liu, S.-S., and Sun, L.-X. (2008). The destabilization mechanism and de/re-hydrogenation kinetics of MgH2-LiAlH4 hydrogen storage system. *J. Power Sourc.* 185 (2), 1514–1518. doi:10.1016/j.jpowsour.2008.09.054

Zheng, J., Liu, X., Xu, P., Liu, P., Zhao, Y., and Yang, J. (2012). Development of High Pressure Gaseous Hydrogen Storage Technologies. *Int. J. Hydrogen Energ.* 37 (1), 1048–1057. doi:10.1016/j.ijhydene.2011.02.125

Zuo, Z., Jiang, W., Qin, X., and Huang, Y. (2020). Numerical Investigation on Full Thermodynamic Venting Process of Liquid Hydrogen in an On-Orbit Storage Tank. *Int. J. Hydrogen Energ.* 45 (51), 27792–27805. doi:10.1016/j.ijhydene.2020.07.099